

AD-A154 436

EVALUATION OF A HIGH PRESSURE PROPORTIONAL COUNTER FOR  
THE DETECTION OF R. (U) AIR FORCE INST OF TECH  
WRIGHT-PATTERSON AFB OH SCHOOL OF ENGI. W LUCYSHYN  
10 MAR 85 AFIT/GNE/PH/85M-15

1/1

UNCLASSIFIED

F/G 18/4

NL

END

FORM 10

2-74



MICROCOPY RESOLUTION TEST CHART  
NATIONAL BUREAU OF STANDARDS-1963-A

AD-A154 436

1



EVALUATION OF A HIGH PRESSURE  
PROPORTIONAL COUNTER FOR THE DETECTION  
OF RADIOACTIVE NOBLE GASES

THESIS

WILLIAM LUCYSHYN  
MAJOR, USAF  
AFIT/GNE/PH/85M-15

Access  
NTIS  
DTIC I  
Unanno

This document has been approved  
for public release and sale; its  
distribution is unlimited.

DEPARTMENT OF THE AIR FORCE  
AIR UNIVERSITY

**AIR FORCE INSTITUTE OF TECHNOLOGY**

Wright-Patterson Air Force Base, Ohio

DTIC  
ELECTE  
JUN 4 1985  
S D  
E

AFIT/GNE/PH/85M-15

DTIC  
ELECTE  
JUN 4 1985  
E

EVALUATION OF A HIGH PRESSURE  
PROPORTIONAL COUNTER FOR THE DETECTION  
OF RADIOACTIVE NOBLE GASES

THESIS

WILLIAM LUCYSHYN  
MAJOR, USAF  
AFIT/GNE/PH/85M-15

Accession For	
NTIS GRA&I	<input checked="checked" type="checkbox"/>
DTIC TAB	<input type="checkbox"/>
Unannounced	<input type="checkbox"/>
Justification	
By	
Distribution/	
Availability Codes	
Dist	Avail and/or Special
A/1	

Approved for public release; distribution unlimited



AFIT/GNE/PH/85M-15

EVALUATION OF A HIGH PRESSURE PROPORTIONAL COUNTER  
FOR THE DETECTION OF RADIOACTIVE NOBLE GASES

THESIS

Presented to the Faculty of the School of Engineering  
of the Air Force Institute of Technology  
Air University  
In Partial Fulfillment of the  
Requirements for the Degree of  
Master of Science in Nuclear Engineering

William Lucyshyn, B.S.

Major, U.S. Air Force

March 1985

Approved for public release; distribution unlimited

## Preface

This thesis is a continuation of two previous studies in an effort to find an adequate system for the analysis of radioactive noble gases using a high pressure proportional counter. Although I discovered the system could not adequately perform this function, the experiment was, nevertheless, a worthwhile learning exercise.

I am deeply indebted to Dr. George John, my thesis advisor, who guided me with unending patience throughout this study. I'd also like to express my gratitude to Bob Hendricks, the lab assistant, and to Carl Short and the rest of the AFIT fabrication shop for their outstanding support, concern, and friendship.

Finally, I owe the most to my wife, Gwendolyn, and to my sons Stefan and Richard, for their patience and support.

William Lucyshyn  
Major, USAF

## Table of Contents

	Page
Preface . . . . .	ii
List of Figures . . . . .	v
List of Tables . . . . .	vi
Abstract . . . . .	vii
I. Introduction . . . . .	1
Purpose . . . . .	1
Background . . . . .	1
Scope . . . . .	3
Approach . . . . .	3
Plan of This Report . . . . .	4
II. Characteristics of the Xenon Gas Sample . . . . .	5
Production . . . . .	5
Xenon 131m and Xenon 133 Decay Data . . . . .	5
Predicted Radioactive Xenon Gas Spectra . . . . .	10
III. Theory of Proportional Detectors . . . . .	11
General . . . . .	11
Multiplication . . . . .	12
Fill Gas . . . . .	14
Resolution . . . . .	18
IV. Equipment . . . . .	24
Gas-Handling System . . . . .	24
The Detector . . . . .	27
The Electronics . . . . .	29
V. Procedures . . . . .	30
General . . . . .	30
Detector Assembly . . . . .	30
Design and Assmebly of the Gas-Handling System . . . . .	32
Operating the Detector System . . . . .	32
VI. Results . . . . .	35
Quench Gas . . . . .	36
Purification . . . . .	37
Multiplication . . . . .	38
Resolution . . . . .	43
Intrinsic Efficiency . . . . .	46
VII. Conclusions and Recommendations . . . . .	52
Conclusions . . . . .	52
Recommendations . . . . .	53

Appendix A: Equipment Calibration . . . . .	56
Appendix B: The External Source . . . . .	60
Appendix C: Sample Spectra . . . . .	61
Appendix D: Resolution Versus Voltage Plots . . . . .	66
Appendix E: Factors Used to Calculate Intrinsic Efficiencies . . . . .	72
Bibliography . . . . .	73
Vita . . . . .	75



# List of Figures

Figure		Page
1	Decay Scheme of $^{131m}\text{Xe}$ . . . . .	8
2	Decay Scheme of $^{133}\text{Xe}$ . . . . .	8
3	Predicted Radioactive Xenon Spectra . . . . .	10
4	Ionization Yield for Argon-Xenon Mixture . . . . .	17
5	The Gas Handling System . . . . .	25
6	The Detector . . . . .	28
7	The Electronics . . . . .	29
8	50 Atm. Argon with 1% Methane . . . . .	36
9	Xenon at 30 Atm. . . . .	37
10	Experimental Multiplication Curves for Argon . . . . .	39
11	Experimental Multiplication Curves for Three Mixtures at 50 Atm. . . . .	40
12	Spectra Taken Over the Center, Left, Then Right Hole .	42
13	Actual Source Well and Model Used . . . . .	47
14	Field Tube Configuration . . . . .	55
15	Argon at 20 Atm. . . . .	61
16	Argon at 30 Atm. . . . .	62
17	Argon at 37 Atm. . . . .	63
18	Argon With .007% Methane at 50 Atm. . . . .	64
19	80% Ar and 20% Xe at 50 Atm. . . . .	65
20	Resolution Vs. Anode Voltage (Ar at 20 Atm.) . . . . .	66
21	Resolution Vs. Anode Voltage (Ar at 30 Atm.) . . . . .	67
22	Resolution Vs. Anode Voltage (Ar at 37 Atm.) . . . . .	68
23	Resolution Vs. Anode Voltage (Ar at 50 Atm.) . . . . .	69
24	Resolution Vs. Anode Voltage (Ar + .007% Methane at 50 Atm.) . . . . .	70
25	Resolution Vs. Anode Voltage (80% Ar + 20% Xe at 50 Atm.) . . . . .	71

### List of Tables

Table	Page
I. Cumulative Fission Yields for Argon . . . . .	6
II. The Effect of Decay Time on the Relative Activity of Noble Gas Mixtures . . . . .	7
III. Characteristic Radiations of Xenon-131m and Xenon-133 .	9
IV. Some Properties of Xenon and Argon . . . . .	15
V. Fill Gases and Pressures Tested . . . . .	35
VI. Experimental Diethorn Constants . . . . .	43
VII. Optimum Experimental Resolution . . . . .	44
VIII. Limiting Theoretical Resolutions . . . . .	45
IX. Parameters for Calculating Geometry Factors . . . . .	47
X. Transmission Factors . . . . .	48
XI. Factors for Theoretical Efficiencies . . . . .	49
XII. Experimental and Theoretical Efficiencies . . . . .	51
XIII. Volumes in Detection System . . . . .	56
XIV. Source Information . . . . .	60

### Abstract

This study evaluates the potential of a newly constructed high pressure proportional counter for the detection of radioactive noble gases. The detector was constructed from stainless steel and machinable ceramic, incorporating design recommendations from a previous study. A new gas handling system was designed and constructed, incorporating a convective flow purification tube filled with calcium turnings.

External sources were used to characterize the performance of the detector using pure argon, argon quenched with varying amounts of methane, a binary mixture (80:20) of argon and xenon, and pure xenon as fill gases. Resolutions were measured as a function of anode voltage and then intrinsic efficiencies were calculated at the optimum resolutions.

A radioactive gas sample was not evaluated when it was found that the field tubes, as designed, did not eliminate the end effects in the detector causing the multiplication to vary along the length of the anode. Consequently, the resolution with an internal sample would not be adequate to perform the required analysis. Additionally, the purification process did not reduce the level of impurities in the available grade of xenon (99.9% pure) to produce useable spectra. Installation of new field tubes, prior to further evaluation of this system, is recommended.

Lackey resumed the testing of this second detector during his research. This detector had a problem with outgassing from the plexiglass insulators (17:96). During his research, a third detector was designed by G. John. Insulators were made from machinable ceramic to eliminate the outgassing problem. Lackey recommended that the work be continued with this new detector (17:100).

#### Scope

The main goal of this research was to continue the study of the characteristics of high pressure proportional detectors. The main concerns are the operating characteristics and energy resolution. In order to be used with the radioactive xenon as an internal source, the detector must have good resolution. When the determination was made that the resolution would not be adequate to analyze a radioactive xenon sample, the scope was further limited to examining the characteristics of the detector at various pressures and with varying gas mixtures.

#### Approach

The first step in this study was to assemble the new detector. Once this was completed, some preliminary 1 atm. tests were made on the existing gas handling equipment. When it was determined that the detector would operate, a new gas handling system, one that would eliminate some of the shortcomings of the existing one, was designed and constructed. Next, volumetric measurements and equipment calibrations were made.

The detector was then tested at 20, 30, 37, and 50 atm. with ultra pure argon as the fill gas. External radioactive sources were used with purified gas as well as unpurified gas.

Next, the effect of using methane as a quench gas with the argon was examined. The methane was added in varying proportions, from less than 0.01% to 5%, to the argon at both 20 and 50 atm.

The xenon portion of the study was begun by evaluating a binary mixture of argon and xenon at 50 atm. as a fill gas. Finally, the study was concluded with an examination of the characteristics of pure xenon.

#### Plan of This Report

The sequence of this report is as follows. The characteristics of the xenon sample are examined in Chapter II. In Chapter III, the theory of proportional counters, including a discussion of multiplication, fill gases, and resolution is presented. Chapter IV contains information about the detection system, and Chapter V outlines the procedures for use of this system. The results obtained, along with an analysis of the results, are presented in Chapter VI. Finally, the conclusions and recommendations of this study are in Chapter VII.

## II. CHARACTERISTICS OF THE XENON GAS SAMPLE

### Production

During a fission chain reaction, numerous xenon isotopes are created. Out of these, four are stable and only three have half lives of sufficient length to study. Table I lists the isotopes, their half lives, and their cumulative fission yields from the fission of  $^{235}\text{U}$ . Table II shows the effect of decay time on the relative activity of the various radioactive species of xenon and krypton.

Of the three isotopes  $^{131}\text{m}$ ,  $^{133}\text{m}$ , and  $^{133}$  with the relatively long half lives,  $^{131}\text{m}$  is produced in such small quantities that it would seem not to be worthy of study. However, with its 12 day half-life it constitutes an increasing amount of total radioactivity of the gas (after 9 days, it constitutes a greater portion than the  $^{133}\text{mXe}$ ). Therefore, during later times,  $^{131}\text{mXe}$  and  $^{133}\text{Xe}$  are the two most logical choices for isotopes to examine to characterize the xenon sample.

### Xenon $^{131}\text{m}$ And Xenon $^{133}$ Decay Data

The metastable state of  $^{131}\text{Xe}$  is 163.72 keV above its ground state. It decays primarily by internal conversion electrons, with a half life of 11.8 days. The decay scheme is shown in Figure 1.

Table I  
Cumulative Fission Yields For Xenon

Isotope	Half-life	Fission Yield (%)
131m	12 days	0.017
131	Stable	2.770
132	Stable	4.130
133m	2.26 days	0.190
133	5.27 days	6.770
134	Stable	7.190
135m	15.7 min.	1.050
135	9.20 hrs.	6.720
136	Stable	6.120
137	3.80 min.	5.940
138	14.2 min.	6.240
139	40.0 sec.	4.960

(20:69)

Table II

The Effect of Decay Time on the Relative Activity  
of Radioactive Noble Gas Mixtures from  $^{235}\text{U}$  Fission\*

---

Percent of Total Activity After Indicated Decay Time					
<u>Isotope</u>	<u>Half-life</u>	<u>2 min</u>	<u>2 hrs</u>	<u>3 days</u>	<u>60 days</u>
$^{139}\text{Xe}$	41.0 sec	3.0			
$^{89}\text{Kr}$	3.2 min	8.2			
$^{137}\text{Xe}$	3.8 min	11.3			
$^{135\text{m}}\text{Xe}$	15.0 min	4.6	0.1		
$^{138}\text{Xe}$	17.0 min	14.1	0.3		
$^{87}\text{Kr}$	1.3 hrs	7.3	5.7		
$^{83\text{m}}\text{Kr}$	1.9 hrs	1.3	1.4		
$^{88}\text{Kr}$	2.8 hrs	10.2	13.5		
$^{85\text{m}}\text{Kr}$	4.4 hrs	4.2	6.7		
$^{135}\text{Xe}$	9.2 hrs	17.2	32.2	0.5	
$^{133\text{m}}\text{Xe}$	2.3 days	0.5	1.0	1.5	
$^{133}\text{Xe}$	5.3 days	18.0	30.0	96.7	2.5
$^{131\text{m}}\text{Xe}$	12.0 days	0.1	0.2	0.8	1.0
$^{85}\text{Kr}$	10.7 yrs	0.1	0.1	0.5	96.5

---

\* From Thermal Neutrons  
(5:76)



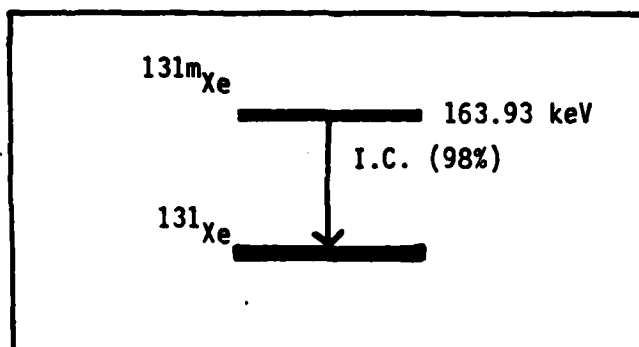


Fig. 1. Decay Scheme of  $^{131m}\text{Xe}$  (18:277)

The radioactive isotope  $^{133}\text{Xe}$  decays by beta emission to an excited state of  $^{133}\text{Cs}$ , 81 keV above the ground state. It has a half life of 5.27 days. This isotope decays principally by internal conversion electrons and gamma rays, with a half life of 6.3 nanoseconds. Figure 2 depicts the decay scheme.

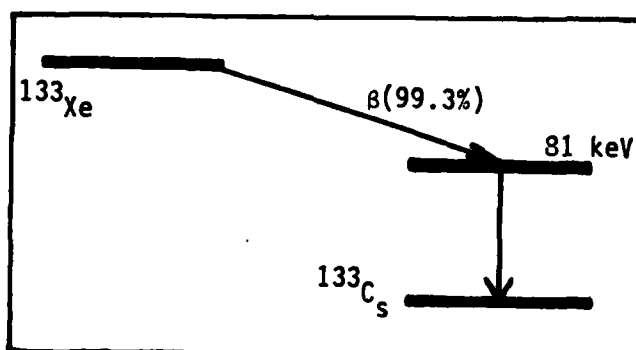


Fig. 2. Decay Scheme of  $^{133}\text{Xe}$  (18:281)

Table III contains detailed decay data of both of these isotopes.

Table III  
Characteristic Radiations of  $^{131m}\text{Xe}$  and  $^{133}\text{Xe}$

Radiation Type	Energy (keV)	Fraction per Decay
$^{131m}\text{Xe}$		
Auger-L	3.43	0.75
Auger-K	24.6	0.068
ce-K	129.369	0.612
ce-L	158.477	0.286
ce-M	162.788	0.0650
ce-NOP	163.722	0.0178
X-ray L	4.1	0.08
X-ray $K_2$	29.458	0.155
X-ray $K_1$	29.779	0.287
X-ray K	33.6	0.102
Gamma	163.722	0.0178
$^{131m}\text{Xe}$		
Auger-L	3.55	0.497
Auger-K	25.5	0.056
ce-K	45.012	0.533
ce-L	75.283	0.081
ce-M	79.780	0.016
ce-NOP	80.766	0.004
Beta - max	346.3	0.993
avg	100.6	
X-ray L	4.29	0.061
X-ray $K_2$	30.625	0.136
X-ray $K_1$	30.973	0.253
X-ray K	35.0	0.091
Gamma	80.997	0.365
(15:138)		

### Predicted Radioactive Xenon Gas Spectra

Lackey predicted the spectrum expected from a mixture of  $^{133}\text{Xe}$  and  $^{131\text{m}}\text{Xe}$  with a total of 5000 counts from the  $^{133}\text{Xe}$  and 50 counts from the  $^{131\text{m}}\text{Xe}$ . Figure 3 below was drawn to reflect a 10 keV resolution for the 164 keV sum peak instead of the 5 keV he used. This would be more realistic with the resolution realizable with this system (17:56).

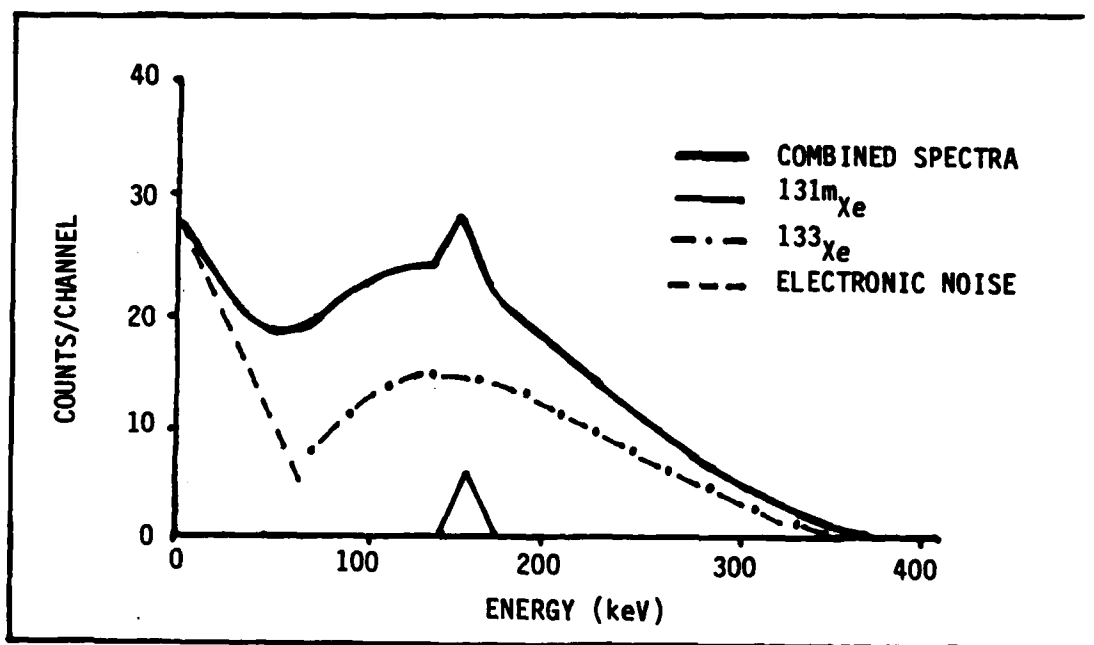


Fig. 3. Predicted Radioactive Xenon Gas Spectra

### III. THEORY OF PROPORTIONAL DETECTORS

#### General

A proportional detector is a type of gas-filled detector that is operated in a voltage region where the output pulse is proportional to the energy deposited by the incident radiation. There is normally a process of gas multiplication so that the output pulse is many times larger than would have been created by the original ion pairs. This gas multiplication is achieved by increasing the electric field between the anode and the cathode. When this field has a low value, the positive and negative ions created by the incident radiation just drift toward the cathode and anode, respectively. When the detector is operating without multiplication, it is said to be operating in the ionization region. As the field is increased, the primary electrons are accelerated to higher velocities. On their path to the anode, they collide with gas molecules, ionizing them and increasing the total number of electrons and positive ions. The secondary electrons, in turn, are also accelerated and ionize other atoms. This cascading effect is known as a Townsend avalanche. At the same time the positive ions, which are much more massive, drift more slowly toward the cathode without causing multiplication. Because of this multiplication process, the electronic system can be operated at lower gain settings, thus improving the overall signal to noise ratio (14:182-183).

### Multiplication

Ideally, the multiplication effect should be independent of where the original ion pairs are formed inside the chamber. This can be achieved by use of a detector with cylindrical geometry. In a cylinder, the electric field at a radial distance  $r$  from the axis is given by

$$E(r) = \frac{V}{r \ln(b/a)} \quad (3-1)$$

where

$V$  = applied voltage

$a$  = anode radius

$b$  = cathode radius

The electric field strength is high in the immediate vicinity of the anode and falls off very rapidly with increasing distance. Now when an ion pair is created anywhere in the sensitive region of the detector (the region where an ionization will cause an avalanche), the electrons will drift toward the anode, accelerating between collisions, until they get within a threshold distance, very close to the anode where they start ionizing the gas atoms. Since the bulk of the charge that produces the signal is localized near the anode, the multiplication will then be independent of where the original ion pairs were created in the detector (14:185-186).

A quantitative expression for predicting the multiplication factor has been derived by several people. One of these, derived by Diethorn, is relatively simple and in reasonable agreement with measurements. In

its derivation he assumes that the only ions formed are through electron collision, that no electrons are lost to form negative ions, and that space charge effects are negligible. With these as assumptions, we can write an expression for the mean multiplication M.

$$\ln M = \int_a^c \alpha \, dr \quad (3-2)$$

where  $\alpha$  is the number of ion pairs formed by one electron per cm. of path length (first Townsend coefficient) and  $c$  is the radial distance from the anode beyond which the electric field is too low to have gas multiplication. The type of gas and the strength of the electric field influence the magnitude of  $\alpha$ . Equation 3-2 can be rewritten

$$\ln M = \int_{E(a)}^{E(c)} \alpha(E) \frac{dr}{dE} dE \quad (3-3)$$

Now if we substitute Equation 3-1 for the strength of the electric field in a cylinder, we can rewrite Equation 3-3 as

$$\ln M = \frac{V}{\ln(b/a)} \int_{E(a)}^{E(c)} \frac{\alpha(E)}{E} \frac{dE}{E} \quad (3-4)$$

Diethorn assumed a linear relationship between  $\alpha$  and  $E$  and derived the relationship

$$\ln M = \frac{V}{\ln(b/a)} \frac{\ln 2}{\Delta V} \left[ \ln \frac{V}{pK a \ln(b/a)} \right] \quad (3-5)$$

where

M = gas multiplication factor

V = applied voltage in volts

a = anode radius in cm.

b = cathode radius in cm.

p = gas pressure in atm.

V = potential difference through which an electron moves between ionizing events in eV.

K = minimum value of E/p in volts/cm-atm below which multiplication cannot occur in volts/cm=atm.

(14:192-193)

Diethorn's assumed relationship is not, however, completely valid over all ranges of voltage and pressure (2:105). The predicted values for multiplication should be viewed as estimates when operating at high pressures and/or high voltages.

### Fill Gas

The multiplication factor in a proportional counter depends on movement of the primary and secondary electrons toward the anode. Consequently, the gases used in these detectors should have minimum electron attachment coefficients (14:190). Noble gases such as argon and xenon have negligible electron attachment and are commonly used. Argon is the most readily available and was chosen as the primary fill

gas for the preliminary testing of this detector. Xenon with its higher x-ray absorption coefficient and higher particle stopping power is the choice for use with the radioactive xenon samples. Xenon is, however, much more expensive (\$18/liter for Xe as opposed to approximately \$.02/liter for Ar) and was used sparingly during the preliminary tests. Table IV shows properties of xenon and argon.

Table IV  
Some Properties of Xenon and Argon

Properties	Xenon	Argon
Triple Point		
Temperature (K)	161.391	83.806
Pressure (torr)	612.2	517.1
Density		
Solid (gm/cc)	3.54	1.622
Liquid (gm/cc)	3.076	1.414
Gas (gm/cc)	8.18	4.04
Liquid		
Boiling Point (K)	165.03	87.27
Density at BP (g/cc)	2.987	1.3998
Atomic Mass	131.3	39.948

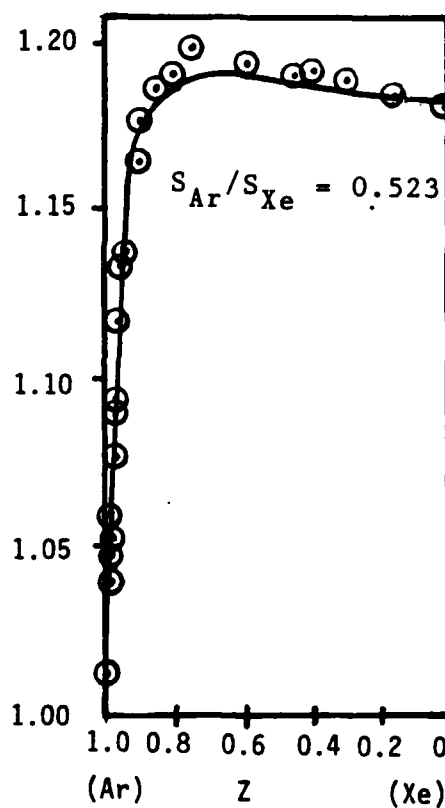
(10:111)



Quench Gases. The addition of polyatomic gases to the fill gas can improve the operation of the detector. In a proportional counter, the secondary electrons, in addition to causing additional ionization, have enough energy to raise the fill gases electron energy levels. De-excitation of these electron states results in the emission of ultraviolet radiation. This radiation can interact photoelectrically with fill gas atoms and initiate a new avalanche which, in turn, can begin the process again with a subsequent rise in the amplification. In the case of the polyatomic gas the electron, over the greatest portion of its path, does not have sufficient energy to cause electronic excitation. The energy is absorbed in inelastic collisions that excite vibrational and rotational energy. This results in the emission of infrared radiation (except in cases near the anode wire). The addition of methane or other polyatomic gases to the basic fill gas can effectively quench the release of ultraviolet radiation by providing a more probable way for lower-energy electrons to lose their energy (22:857-858). When the detector is operated with a multiplication factor below approximately 100, noble gases in pure or binary form can be successfully used (24:389).

Noble Gases In Combination. Increasing the ionization yield of the primary fill gas is possible by addition of a small amount (about 0.01%) of a second gas. This is known as the Jesse effect. The ionization energy of the added gas should be lower than both the ionization energy and the metastable energy levels of the primary gas. Now, collisions between the excited primary gas atom and the additive gas atom result in the ionization of the additive gas atoms. If, on the other hand, a second gas with an ionization energy higher than the excitation energy

of the primary gas is added in larger amounts, the number of ionizations will also be increased. It is suggested that this is possible because the non-metastable states in the primary gas, which are higher than the ionization energy of the additive gas, persist long enough to allow collisions and subsequent ionization of the additive gas atom. This process is known as the non-metastable Penning process (16:1017). The effect on the ionization yield of combining argon and xenon in different proportions can be seen in Figure 4.



$$Z = [1 + (S_{Xe}P_{Xe}/S_{Ar}P_{Ar})]^{-1}$$

Figure 4. Ionization Yield For Argon-Xenon Mixture (16:1022)

Electronegative Impurities. Electronegative impurities present in the fill gas have an adverse effect on the characteristics of the detector. These impurities are either present in the gas filling at the beginning of the measurement or evolve from materials and micro cracks in the detector during the measurement. These impurities have two possible consequences. They can capture primary electrons reducing the overall charge collected or they can reduce the electron drift velocity. A lower drift velocity causes additional losses of primary electrons by attachment processes. Impurities with a high electron affinity, e.g., halogens, water vapor, and oxygen have the most effect. Additionally, as the pressure inside the detector increases, the sensitivity to the electronegative impurities in the fill gas also increases. Therefore minimizing these impurities, especially in high pressure operations, is necessary to improve the overall characteristics of the detector (21:363-368).

#### Resolution

A common measure of the resolution, of a proportional counter, is the full width at half maximum (FWHM) of the distribution of output pulses produced by a monoenergetic source. Two factors influence the resolution of a detector. One is the statistical process of the pulse formation. The other is the practical design of the detector (electronic noise, anode wire eccentricity and uniformity in diameter, end effects, and other factors of lesser importance) (25:230).

Statistical Consideration. Statistical variation of the pulse height is a prime consideration since it is, in principle, the fundamental limit to the resolution and cannot be eliminated. The

fluctuations in the charge  $Q$ , which is developed in a pulse from a proportional counter, depend on the variance of the primary ionizations and the gas multiplication in the following way.

$$\left(\frac{\sigma_Q}{Q}\right)^2 = \left(\frac{\sigma_{n_0}}{n_0}\right)^2 + \frac{1}{n_0} \left(\frac{\sigma_A}{A}\right)^2 \quad (3-6)$$

where  $n_0$  is the number of ion pairs created

$A$  is the mean amplification or multiplication factor

$\sigma_Q, \sigma_{n_0}, \sigma_A$  are the standard deviations of the previous quantities (14:197).

The first term on the right hand side of this equation represents the variation of the original number of ion pairs,  $n_0$ . This variation follows the dependence described by Fano

$$\left(\frac{\sigma_{n_0}}{n_0}\right)^2 = \frac{F}{n_0} \quad (3-7)$$

where  $F$  is a constant, characteristic of the particular fill gas and  $\sigma_{n_0}$  is taken as  $(n_0)^{0.5}$ , as if it were a Poisson distribution. The constant  $F$  is known as the Fano factor (7:26-29). The second term on the right hand side describes the variation in the magnitude of a single electron avalanche. If a Polya distribution is used to describe the distribution in the number of electrons produced in a given avalanche, the variance predicted is

$$\left(\frac{\sigma_A}{A}\right)^2 = \frac{1}{A} + b \quad (3-8)$$

where  $b$  is a factor related to the number of electrons that exceed the threshold energy required for ionization. It is constant for a specific fill gas. For a large mean amplification, Equation 3-8 reduces to

$$\left(\frac{\sigma_A}{A}\right)^2 = b \quad (3-9)$$

Substituting Equation 3-7 and Equation 3-9 into Equation 3-6, the resultant variation in the charge,  $Q$ , is

$$\left(\frac{\sigma_Q}{Q}\right)^2 = \frac{F}{n_0} + \frac{b}{n_0} \quad (3-10)$$

or

$$\left(\frac{\sigma_Q}{Q}\right)^2 = \frac{1}{n_0} (F + b) \quad (3-11)$$

The number of primary ions  $n_0 = \frac{E_{\text{dep}}}{W}$ , where  $E_{\text{dep}}$  is the energy deposited by the radiation and  $W$  is the average energy required to form one ion pair. Then

$$\left(\frac{\sigma_Q}{Q}\right)^2 = \frac{W}{E_{\text{dep}}} (F + b)$$

If one assumes that each monoenergetic particle deposits all of its energy and that the distribution is normal, this variance can be expressed in terms of the FWHM in keV where

$$\text{FWHM} = 2.36[(F+b) E_{\text{dep}}W]^{0.5} \quad (3-14)$$

End Effects. In order for the multiplication effect to be constant throughout the sensitive volume, the electric field must be constant in that region. A serious degree of distortion to the electric field is introduced by the end supports and end plates of the detector. This distortion can extend the sensitive volume beyond the end of the anode wire and create a region in the detector, about one cathode radius in length, in which the multiplication factor rises slowly to a constant value at a large distance from the support. Although not used in this detector design, small field tubes can be fitted around the anode wire and maintained at an appropriate voltage. These would reduce the end effects to negligible proportions and create a well-defined sensitive volume (6:37-38). The voltage to be applied to the field tube  $V_p$  is found from the following relationship

$$V_p = \left[ \frac{\ln(r_p/r_w)}{\ln(r_c/r_w)} \right] V_c \quad (3-14)$$

where  $V_c$  = the cathode voltage

$r_p$  = the radius of the field tube

$r_w$  = the radius of the anode wire

$r_c$  = the radius of the cathode (6:38)

An alternate to the field tube is to use supports for the anode wire at each end that are slightly larger than the anode wire. Thus the variation in the field is reduced, and its magnitude is dropped sufficiently to prevent multiplication from occurring. This approach was used in the current design in order to simplify the design and eliminate the need for a second power supply.

Other Factors. Other factors exist which affect the resolution of a proportional counter and, in general, degrade it from the value predicted by the statistical limit. These factors fall into three categories: electronic noise, geometric nonuniformities, and variations in detector operating parameters. Noise levels available with modern solid state electronic equipment are generally low enough not to have a significant impact on the resolution (14:201-202).

Geometric nonuniformities can have a significant impact on the detector's resolution. The most critical are end effects (previously discussed) and variations as small as .5% in the anode diameter. In the present design, with an anode diameter of 0.0003 in.  $\pm$  02%, the variation in the multiplication factor is  $\pm$  15% (calculated using the Diethorn relationship). Other geometric factors, e.g., the eccentricity of the wire and the nonuniformity of the cathode, are less critical (14:202).

The resolution of the proportional detector is also significantly affected by changes in operating parameters. Small pressure changes (as small as a few tenths of one percent) can have a significant effect (14:202). In high pressure operation, however, the gas pressure will be fairly constant if the system is free from leaks. Small variations in

voltage can also have a significant effect on the multiplication and, consequently, the resolution. Therefore, it is important to use well-regulated power supplies that are free from long term drifting (14:203). The effect of electronegative impurities has been previously discussed. Finally, resolution can be adversely affected by pulse saturation. This can be caused by either high-energy photons at high gas multiplications or excessive count rates. Using large diameter anode wires and low count rates can alleviate this effect (4:209). However, when an anode wire with a large diameter is used, the voltage needed to get multiplication becomes excessive.



#### IV. EQUIPMENT

The equipment used in this experiment is divided into three categories for ease of description and visualization. These are the gas-handling system, the detector, and the electronics.

##### Gas-Handling System

The first part of the detection system is the gas-handling system. This system consists of two sections: the vacuum pumping section and the gas filling section. The purposes of this system are to evacuate the detection system to low vacuum pressures, introduce the appropriate amount of fill gas, and then purify it. Figure 5 shows a schematic of how the gas-handling system is arranged.

The Pumping Section. The vacuum pumping section consists of a forepump and a diffusion pump with cold trap. A Penning type vacuum gauge is located on the system side of the diffusion pump. It has a range from  $25 \times 10^{-3}$  torr to  $10^{-8}$  torr. The forepump can evacuate the detection system down to  $10^{-3}$  torr in approximately 5 minutes. Then with the diffusion pump running, the pressure can be brought down to  $10^{-7}$  torr in an additional 40 minutes. The diffusion pump has a locally manufactured cold trap that is filled with liquid nitrogen. There is also a continuous feed dewar connected to the cold trap that holds a two day supply of liquid nitrogen (approximately 20 liters). Standard vacuum valves are used to connect the vacuum pumping section to the rest of the system and to bypass the diffusion pump when required.

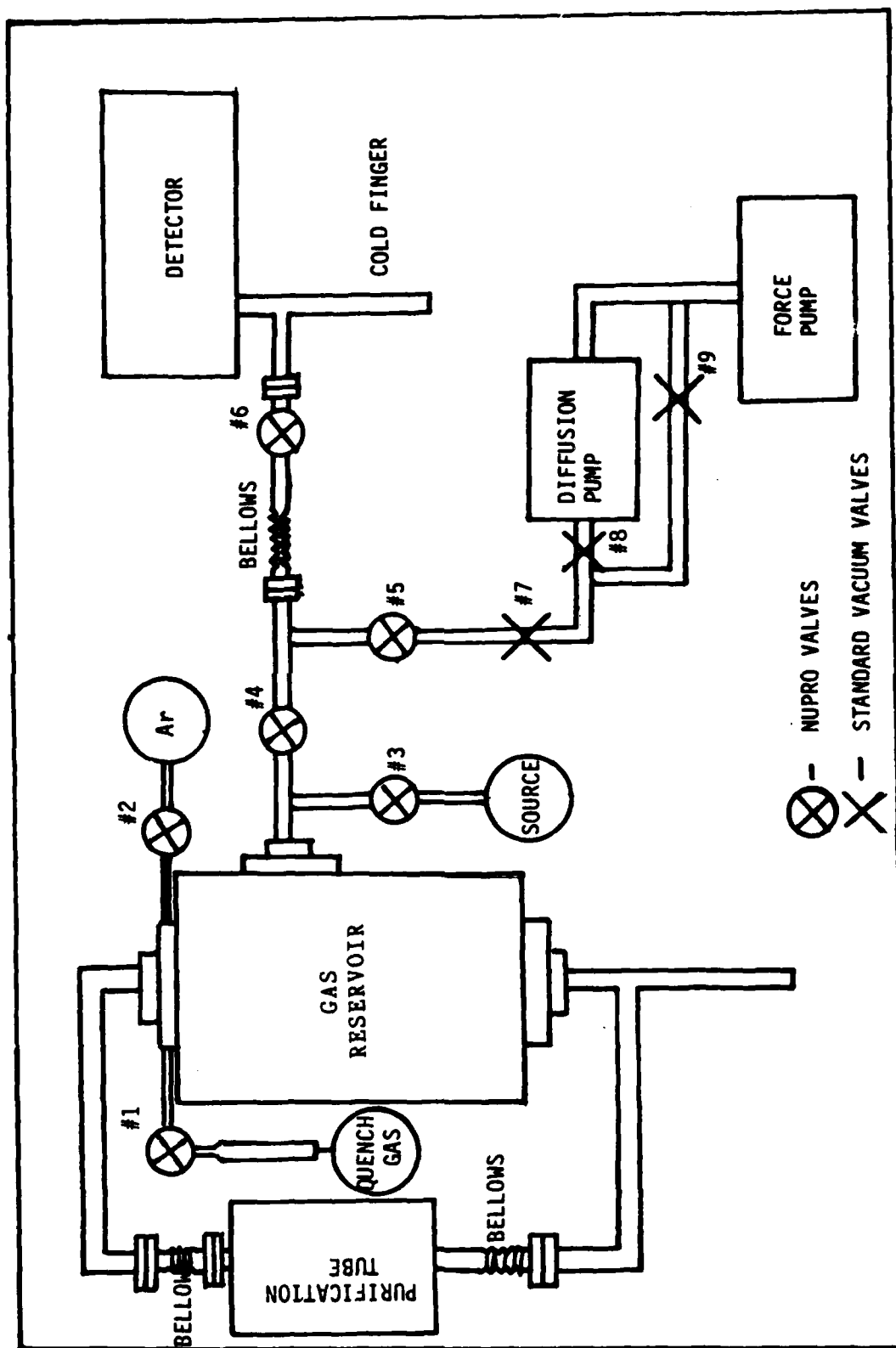


Figure 5. The Gas-Handling System

The Filling Section. The filling section consists of a gas reservoir with provisions to pump in the fill gas, the radioactive sample, and a quench gas, and the purification tube. There is also provision to cryogenically pump the fill gas and sample back into the reservoir. The reservoir is a modified commercially-constructed steel gas cylinder with Varian type flanges silver soldered to the top, bottom, and side to facilitate connections to the purification tube, pumping section, and detector. The fill gas and quench gas inlets (valves 1 and 2), as well as a Pace pressure transducer, are silver soldered into the top Varian type flange. A stainless steel cylinder filled with dreirite is connected at the quench gas inlet. Another stainless steel cylinder (cold finger) for cryogenic backpumping is connected to the bottom of the gas reservoir. The inlet for the radioactive gas sample (valve 3) is connected to the side of the reservoir with a stainless steel adapter to accept glass break seal tubes. Valve 4 connects the filling section with the pumping section and detector. The purification tube consists of a quartz tube passing through a tubular oven. The quartz tube has a graded seal (attached to stainless steel tubing) at both ends. Stainless steel bellows are connected at both the top and bottom of the tube to facilitate installation. The tube is mounted vertically, with Varian flanges, to 0.5 in. O.D. stainless steel tubing, on the side of the gas reservoir. The quartz tube is filled with calcium metal turnings (9:224) and heated with an electric resistance furnace. A thermocouple, attached at the center of the tube, is connected to a temperature indicator to monitor the temperature.

### The Detector

The detector, depicted in Figure 6, is constructed from a stainless steel cylinder 6.25 in. long, with an O.D. of 3.360 in. and an I.D. of 1.625 in. The end plates are made of 0.625 in. stainless steel. They are attached to the body with bolts and sealed with Varian-type knife-edge seals and a soft copper ring. The detector is designed to withstand pressures greater than 50 atmospheres. There is a removable section made from machinable ceramic end pieces and three stainless steel rods. This section holds the wire support/field tubes and the anode wire with a spring tensioner. The center section can be removed, with the removal of the right end plate, to facilitate replacement of the anode wire. Electrical contact to the outside is made with brass contacts epoxied to ceramic insulators, which are epoxied to the end caps. High vacuum epoxy was used throughout assembling the components. The anode wire used is 0.0003 in. diameter 304 stainless steel. The body of the detector also has three 3/16 in. diameter holes drilled in its side to a depth of 0.835 inches for use with external sources. A stainless steel cold finger, used for cryogenic pumping of fill gas (for high pressure operations), is fastened by pipe threads and epoxied on the inside surfaces of the detector, to minimize outgassing. The detector is connected to the rest of the system with a Varian flange. There is a glass tube inserted to the left of valve 6 to electrically isolate the detector from the rest of the system so the cathode could be operated at a negative high voltage if required.

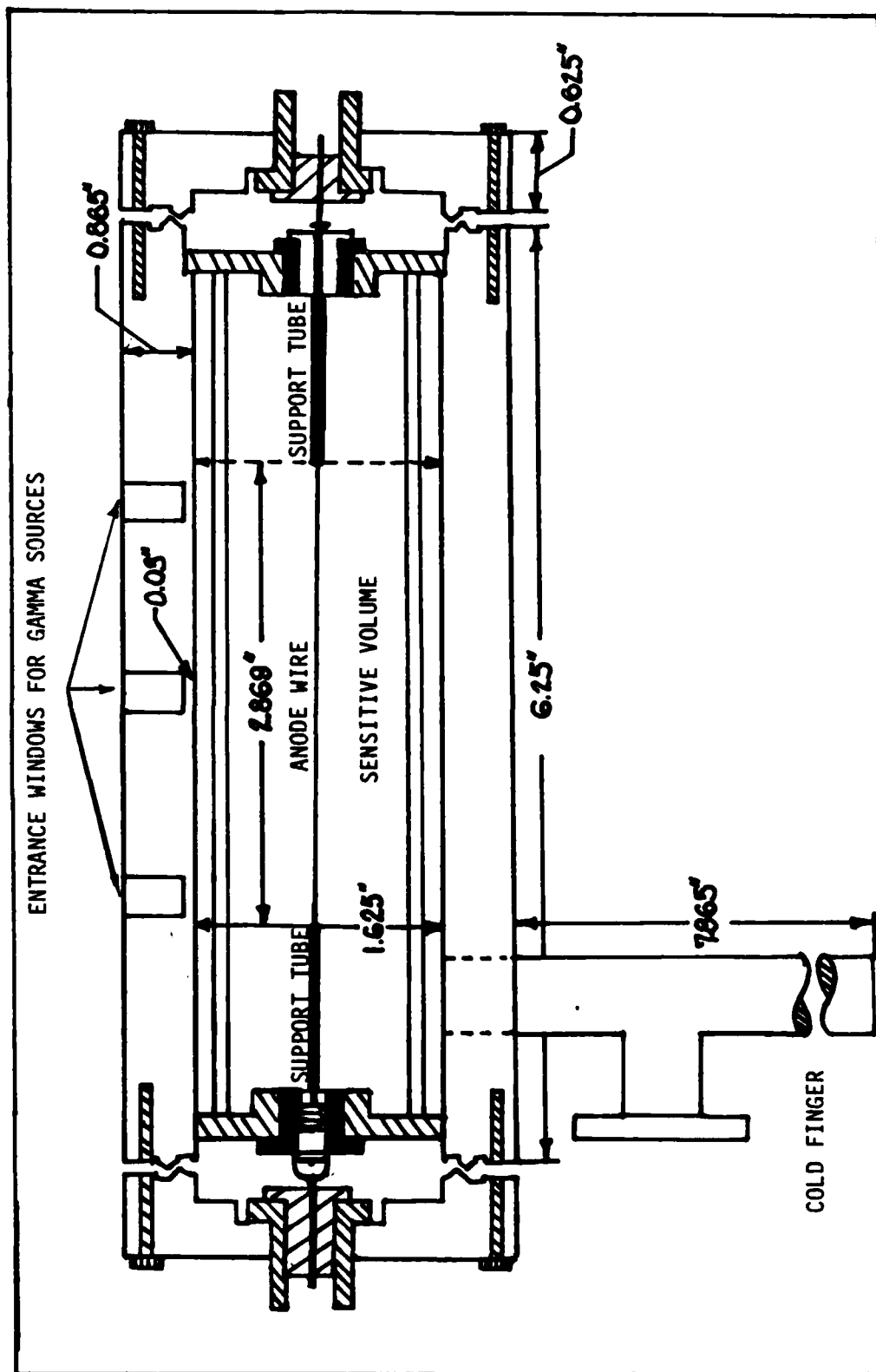


Figure 6. The Detector

### The Electronics

The electronics are of the standard type used with proportional detectors and are schematically shown in Figure 7. The pulse of charge from the anode is converted to a voltage pulse by a preamplifier. This voltage pulse is amplified and shaped by a linear amplifier. The signal from the linear amplifier is then monitored on an oscilloscope and analyzed with a multichannel analyzer. Additionally, the signal from the linear amplifier is fed into a single channel analyzer and to a timer/scaler for counting integral output. The bias voltage to the anode is supplied by a high voltage power supply with maximum output of 5000 volts (stable within 50 ppm per hour).

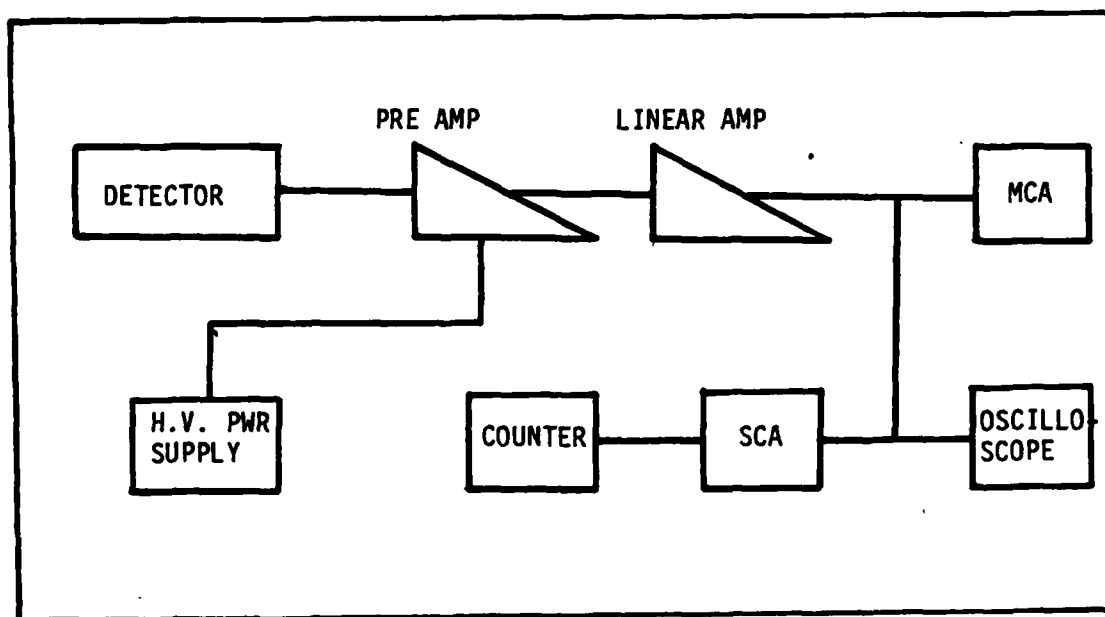


Fig. 7. The Electronics

## V. PROCEDURES

### General

There were three phases to this experiment. The first phase was assembling the detector. The main emphasis here was to clean the parts thoroughly and maintain them as contaminant free as possible. The second phase was designing and constructing the gas-handling system. The primary consideration here was to design the system to incorporate a convective flow through the purification tube and, at the same time, minimize cracks and crevices to preclude the introduction of impurities into the fill gas. The final phase was obtaining spectra with the detector using different fill gas mixtures at various pressures with external sources.

### Detector Assembly

Before the actual assembly, all of the parts were cleaned of dirt, machine oil, and any other contaminants. First, trichlorethelene and a bristle brush were used to scrub all of the parts. Next, the parts were placed in a bath of ISOCLEAN solution and heated at 50° C for three hours. Then the parts were removed and thoroughly rinsed with tap water and then with distilled water. Finally, they were cleaned again with ethyl alcohol. The ceramic parts were then placed under vacuum and heated to 85° C for three hours to outgas as much of the water adsorbed gases as possible. The parts were then kept in a clean dessicator containing dreirite as a dessicant, until assembly.

The assembly process was begun by bonding the insulators and the connectors to the end plates with a high vacuum grade epoxy made by Varian. The epoxy was mixed in small plastic bags in an effort not to mix any air into it. The epoxy was then applied to one of the surfaces and heated with a hot air gun for approximately 30 seconds. The facing parts were then pressed together. The joint was heated again to form a smooth bead. The center section was assembled using the same procedure with the epoxy. The cold finger was threaded into the body of the detector and then epoxied on the inside to cover the thread line. When the center section had cured, a 0.005 in. stainless steel wire lead was threaded through it. The anode wire was then attached to this lead with cyanoacrylic. The lead was then carefully pulled through the center section. The anode wire was attached at the left end (the end with the smaller diameter ceramic plate) with a brass pin and a drop of cyanoacrylic. The anode wire was tensioned with approximately 2 gms. and the right hand pin was inserted very gingerly, since too much pressure would break the fine anode wire. The center assembly was then placed under vacuum, and the anode "glowed" with a 10 milliamp current. The final assembly was accomplished by bolting on the left end plate (the end closer to the cold finger), inserting the center section, and bolting on the right end plate. The detector was mounted in its holder and connected to the existing gas-handling system, used by Knapp and Lackey, with a Varian flange. Pressure in the system was now reduced to, and kept at, approximately  $10^{-7}$  torr.



### Design And Assembly of The Gas-Handling System

A new gas-handling system was constructed to incorporate Lackey's recommendation (17:98) of a convective flow purification section and to replace the locally constructed gas reservoir with a commercially manufactured gas cylinder. The system was also designed to minimize the number of connections. Additionally, special valves with bellow seals were purchased. All required connections were either silver soldered or made with Varian or Varian type flanges with soft copper rings. Required silver soldered joints were made so the solder flowed inside to form a bead without crevices. When the soldering was complete, the components were cleaned in a hot water bath to remove any remaining flux. They were then rinsed with trichlorethelene and ethyl alcohol. The components were then assembled and connected to the vacuum system. An aluminum foil reflector oven, using three 250 watt infrared lamps as a source of heat, was constructed around the gas-handling system. The temperature was raised to approximately 80° C and kept there for 24 hours while the system was under vacuum to facilitate outgassing. The detector was now connected to the new gas-handling system. The entire detector system was now evacuated down to a pressure of  $10^{-7}$  torr.

### Operating The Detector System

General. There are five procedures in the operation of this detection system. They are charging the system, purification of the fill gas, pressurizing the detector, introducing the radioactive sources, and collecting data.

Charging The System. This first procedure prepares the gas-handling system and fills the reservoir with the required amount of fill gas. First, the system is evacuated with the forepump and diffusion pump down to a pressure of  $10^{-7}$  torr. If the purification procedure is to be used, the purification material is heated to  $650^{\circ}\text{C}$  and allowed to outgas for 8 hours. The system is now flushed with 99.999% pure Argon. This is accomplished by filling the system to a pressure of 200 mmHg. The diffusion pump is then bypassed and the system is pumped down to  $10^{-3}$  torr. Now, the diffusion pump is used to pump the system down to below  $10^{-5}$  torr. This process is repeated three times. Finally, the fill gas is fed into the reservoir to the required pressure reading. This pressure is calculated using Van Der Waal's equation so that when the gas is transferred into the detector, the desired operating pressure is achieved.

Purification. When the system is charged with the appropriate amount of fill gas, it is a relatively simple matter to purify it, if necessary. The temperature of the tubular oven is raised to heat the calcium turnings inside the purification tube to  $650^{\circ}\text{C}$  ( $9:224$ ). Since this tube is aligned vertically beside the reservoir, the convective flow circulates the fill gas through the purification tube. The gas is allowed to purify overnight in this manner.

Pressurizing The Detector. When the fill gas is ready, it is cryogenically transferred into the detector. The detector is kept under vacuum ( $10^{-7}$  torr) until immediately before the transfer. The pumping section is then isolated and the fill gas is allowed to expand into the detector. A dewar of liquid nitrogen is slowly raised over the detector cold finger. When the gas condenses in the cold finger and the pressure

drops to the vapor pressure of the gas at liquid nitrogen temperature, the valve isolating the detector from the rest of the system is closed. The vapor which remains in the system and does not condense is taken into account. The dewar of liquid nitrogen is lowered and the cold finger raised to room temperature, expanding the gas in the detector.

Introducing The Radioactive Sources. The detector was designed to be tested with external sources and operate with a radioactive xenon gas sample introduced internally. The external sources are normally fixed to plexiglass disks and are placed over one of the three source windows in the top of the detector (see Figure 6). The radioactive xenon gas contained in a break seal tube is introduced at the source gas connection. A dewar of liquid nitrogen is raised over the gas reservoir cold finger to cryogenically pump the xenon from the break seal tube into the reservoir. Once all the gas is transferred, the valve at the source gas connection is closed. The fill gas is now added and the source expanded in the reservoir. The gas is now purified and handled as described previously. The radioactive xenon can be cryogenically transferred back to the reservoir and then into a gas cylinder and connected at the source gas inlet at the end of the counting.

The Collection Of Data. Once the fill gas is expanded in the detector and the sources introduced, the system is ready to collect data. The anode voltage is set while monitoring the pulses on an oscilloscope. The spectra are then analyzed with a multichannel analyzer and recorded on 8 inch computer diskettes.

## VI. RESULTS

This research was a continuation of two previous studies of high pressure proportional counters. The system used, however, was newly built. Therefore, prior to characterizing the detector's response there was a requirement to measure the volumes in the gas handling system and calibrate the equipment. See Appendix A for calibration details. Once these preliminary measurements were done, the response of the detector was studied using external sources (see Appendix B for data on sources used) and the combinations of fill gases and pressures shown in Table V.

Table V  
Fill Gases and Pressures Tested

Gas Mixture	Pressure (Atm)			
	20	30	37	50
Argon	X	X	X	X
Argon + 0.007% Methane				X
Argon + 0.01% Methane				X
Argon + 0.1% Methane	X			X
Argon + 1% Methane	X			X
Argon + 5% Methane	X			X
80% Argon + 20% Xenon				X
Xenon		X		
Xenon + 0.01% Methane		X		

The signals were monitored on the oscilloscope and as soon as distinct pulses were visible, spectra were collected with the MCA. The anode voltage was then raised in increments of 100 volts until the detector began discharging. See Appendix C for sample spectra. Although an effort was made to collect spectra with xenon at 50 Atm., it was unsuccessful. The anode voltage required exceeded the 5000 volts available with the HV power supply.

#### Quench Gas

Although different amounts of quench gas were mixed with the argon, the only combination that worked satisfactorily was argon mixed with 0.007% methane. This was enough methane to quench the argon and allow operation at a higher anode voltage, without adversely affecting the spectra. When more than this amount was added, there was a broadening of the photo peak with what appeared to be a Compton tail. See Figure 8 for a typical example.

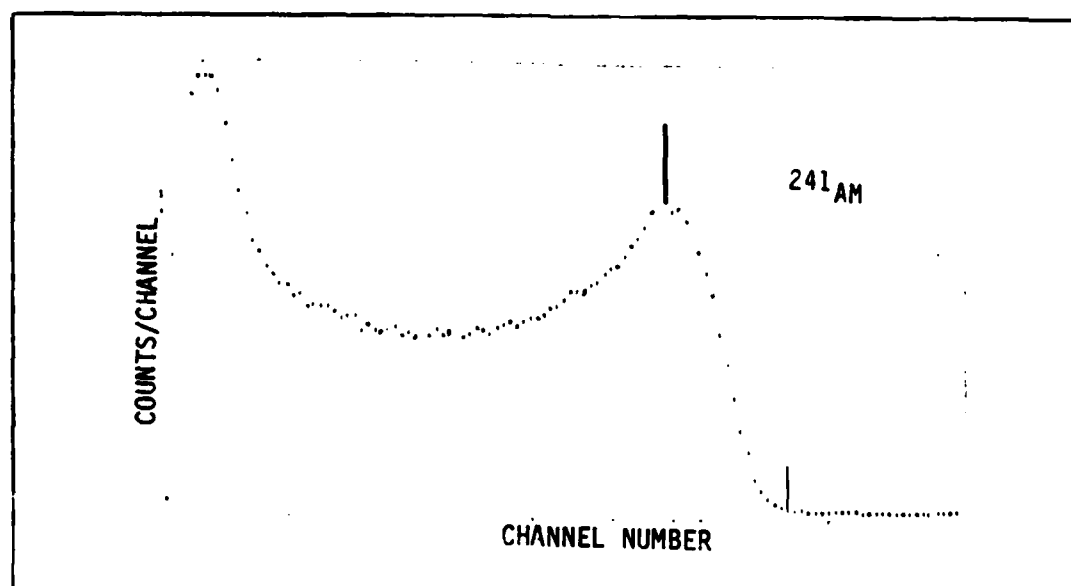


Figure 8. 50 Atm. Argon With 1% Methane at 3800 Volts

### Purification

The purification through the calcium only had an effect on the results when xenon was used. The level of impurities in the ultra pure argon (99.999% pure) was evidently below the threshold of what the calcium would remove. There was no improvement in the argon spectra after purification.

The xenon, on the other hand, was only 99.9% pure. The results of the argon-xenon mixture were unusable unless the gas was first purified. The pure xenon produced a spectrum only after purification, but the resolution was not good enough to distinguish the xenon escape peak from the full energy peak (approximately 30 keV). See Figure 9 for a sample spectrum. The results with the xenon-methane mixture were the same.

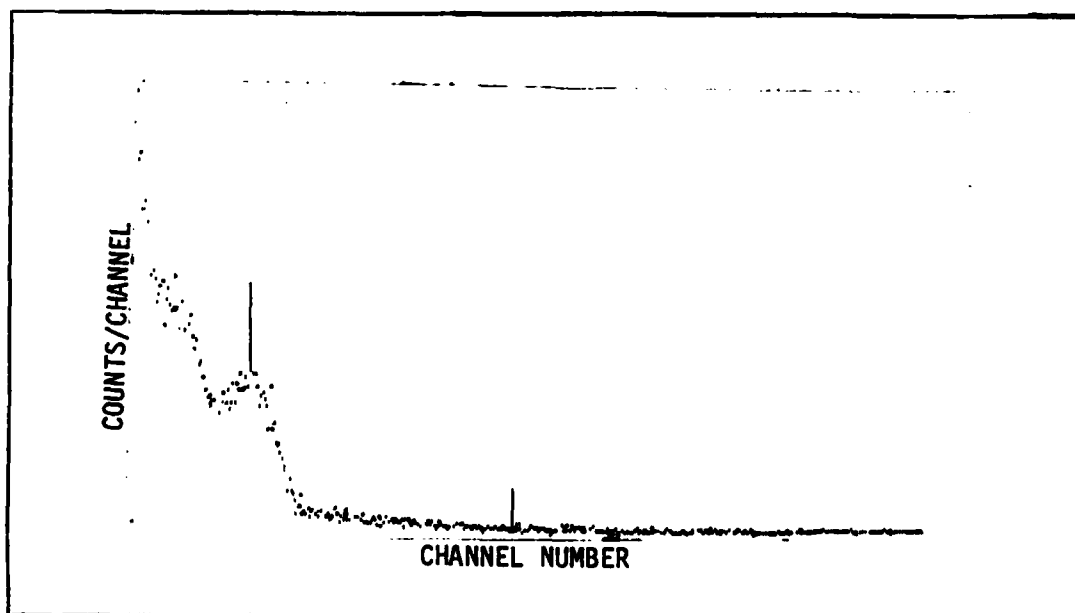


Figure 9. Xenon at 30 Atm. and 3900 Volts. Source is  $^{241}\text{Am}$ .  
Xe purified for 12 hours.

### Multiplication

Once the spectra were collected, the multiplication factors could be calculated directly using the following relationship

$$ph = Q M G_{pa} G_{la} \quad (6-1)$$

where  $ph$  = pulse height in mV  
 $Q$  = charge deposited in pC  
 $M$  = the multiplication  
 $G_{pa}$  = the gain of the pre amp in mV/pC  
 $G_{la}$  = the gain of the linear amp

and

$$Q = (E_{dep}/W)e \quad (6-2)$$

where  $E_{dep}$  = energy deposited  
 $W$  = energy expended per ion pair in eV  
 $e$  = charge per ion pair in pC

To test if the pressure inside the detector was remaining constant, the detector was pressurized and allowed to remain that way for 48 hours. When the pressure was vented back into the system, the pressure returned to the same value used at the time of filling. The pressure, therefore, was assumed to remain constant for the period of data collection, which was never more than 8 hours, after pressurization. Experimental multiplication curves for argon at different pressures are depicted in Figure 10 and for the three gas mixtures that produced spectra with distinct and recognizable peaks at 50 Atm. in Figure 11.

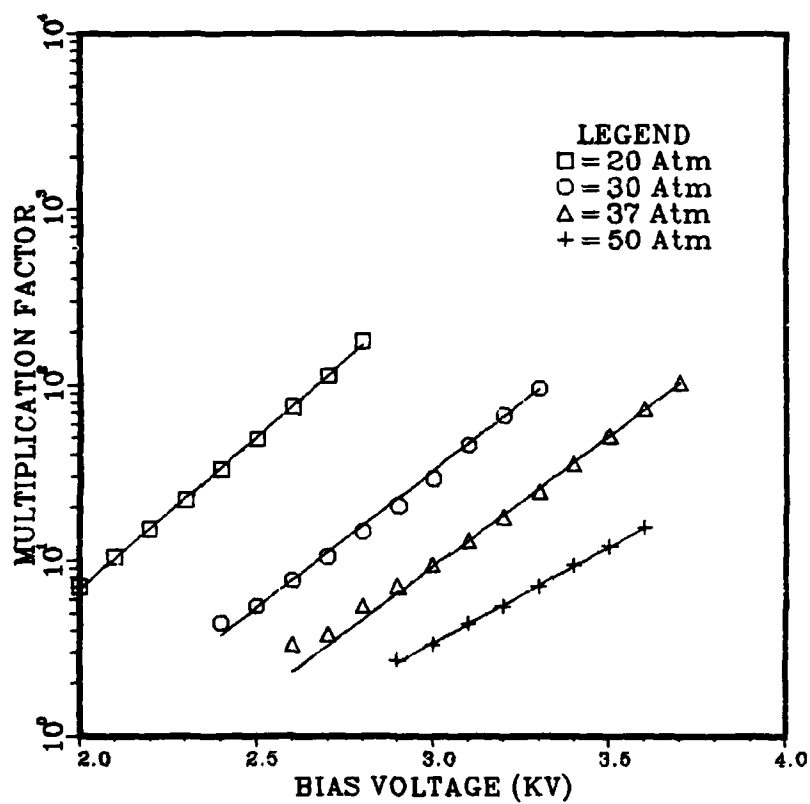


Figure 10. Experimental Multiplication Curves for Argon



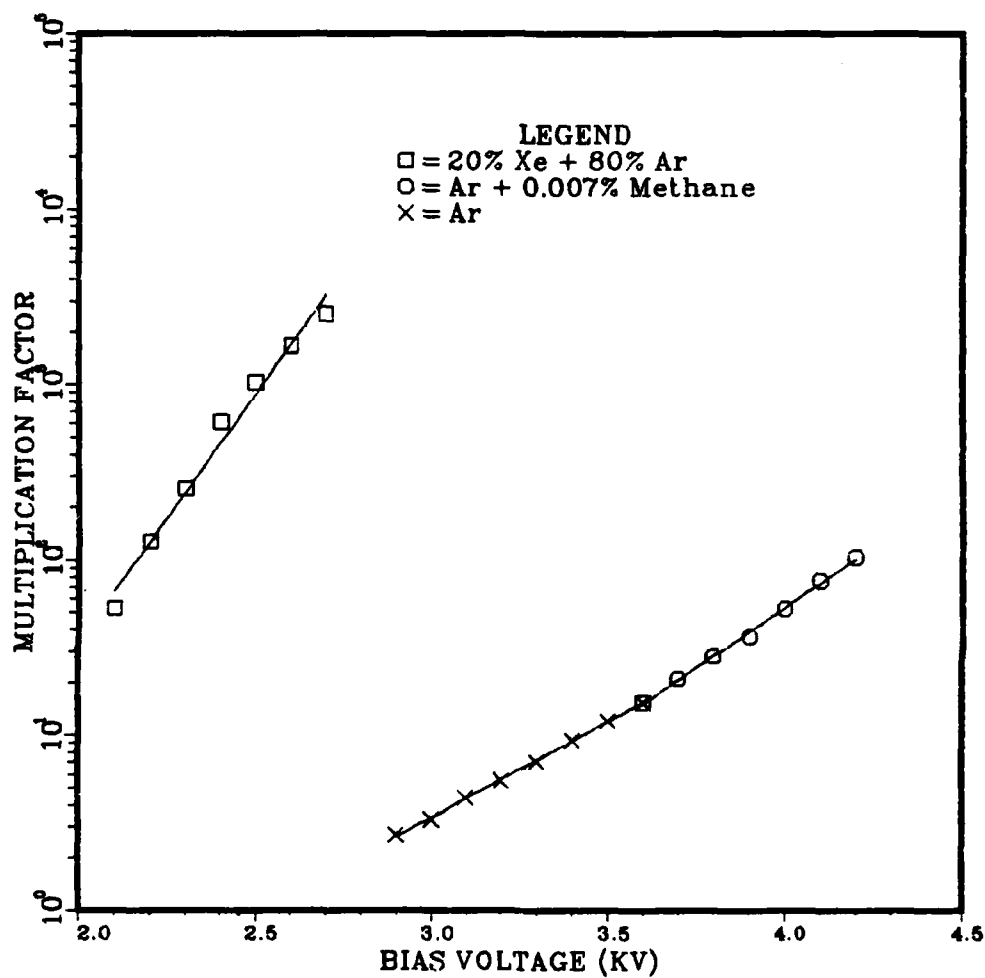


Figure 11. Experimental Multiplication Curves for Three Mixtures at 50 Atm.

These spectra were all collected with the source over the center hole. When a check was made to see if the multiplication was uniform along the length of the anode, it was found that the field tubes, as designed, were not working. The left and right holes produced peaks with different multiplication factors. Equation 3-1 was used to calculate the electric field at a point 0.40525 inches above the detector centerline with 4000 volts applied to the anode. The field calculated above the anode was 449 volts/cm as opposed to 1013 volts/cm above the support tube. This distortion of the field produced the undesirable end effects. Figure 12 shows an example of this phenomenon with an argon + 0.007% methane mixture at 50 Atm.

Once the multiplication factors were known, the Diethorn relationship could be used to calculate the Diethorn constants,  $\Delta V$  and  $k$ . This is done by manipulating Equation 3-5 into the following form

$$\frac{\ln M \ln(b/a)}{V} = \frac{\ln 2}{\Delta V} \cdot \ln \left[ \frac{V}{p a \ln(b/a)} \right] - \frac{\ln 2 \ln k}{\Delta V} \quad (6-3)$$

Now if  $V/\ln[p a \ln(b/a)]$  is plotted on the x axis and  $[\ln M \ln(b/a)]/V$  is plotted on the y axis for a number of different voltages, the slope is obviously  $\ln 2/\Delta V$  and the intercept is  $-\ln 2 \ln k/\Delta V$ . Now  $\Delta V$  and  $k$  can readily be found. A least squares fit was used to find both the slope and the intercept. Table VI has the experimental Diethorn constants.

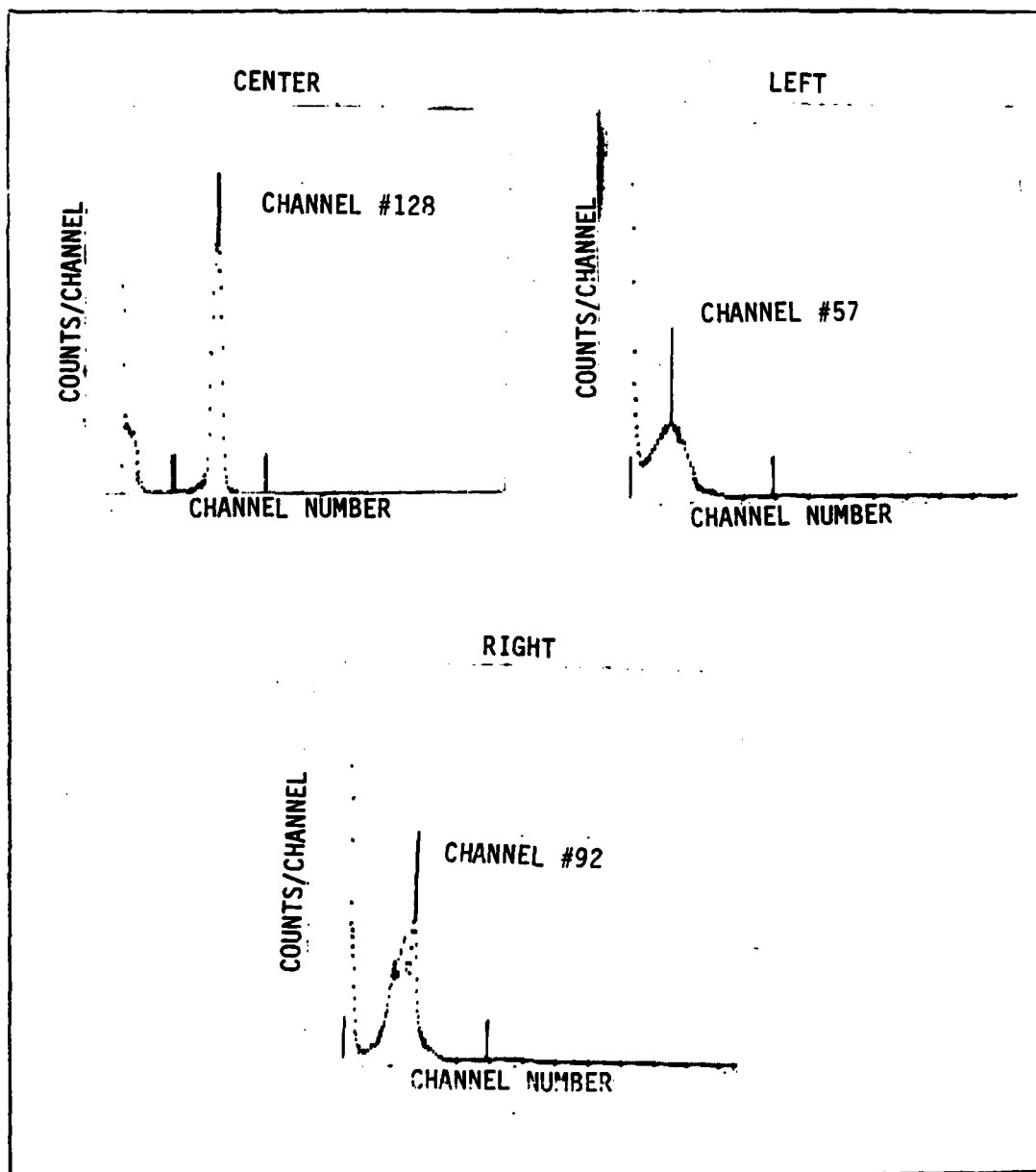


Figure 12. Spectra Taken With the  $^{241}\text{Am}$  Source Over Center, Left, Then Right Hole (Anode at 4100 Volts)

Table VI  
Experimental Diethorn Constants

Gas	Pressure	V(eV)	k (V/cm-atm)
Ar	20	31.5	20,729
Ar	30	32.7	19,244
Ar	37	34.8	17,838
Ar	50	40.8	14,915
Ar + 0.007% Methane	50	36.2	15,654
80% Ar + 20% Xe	50	19.9	7,806

There are no constants available in the literature for comparison with these except the ones Lackey calculated for pure argon. His experimental values for  $\Delta v$  and  $k$  were 28 eV and 14,500 V/cm-atm respectively for argon at both 25 and 50 atm. (17:80).

#### Resolution

As discussed in Chapter III, resolution is defined in terms of the peaks FWHM and expressed in energy units (keV). It can also be expressed in terms of percent by dividing both sides of Equation 3-4 by the energy deposited.

$$R(\%) = 2.36 [(F+b)W/E_{dep}]^{0.5} \quad (6-4)$$

In an effort to find the optimum operating conditions, the resolution was measured at various anode voltages. The voltages were increased until a discharge in the detector precluded any more collection. The results were then plotted and the voltage with the best resolution was chosen as the optimum voltage for that particular gas and pressure. See Appendix D for the plots. The resolutions plotted were not corrected for the noise generated by the electronic equipment in the system. In the range of operation of this experiment, the noise was determined to be 2 channel FWHM by measuring the resolution of the pulser signals used to calibrate the MCA. Table VII shows the optimum resolutions adjusted for the electronic noise.

Table VII  
Optimum Experimental Resolutions

Gas	Pressure (Atm.)	Voltage (KV)	Resolution (%)		
			<sup>241</sup> Am	<sup>109</sup> Cd	<sup>57</sup> Co
Ar	20	2.8	12.8	10.3	14.8
Ar	30	3.2	9.8	6.7	11.9
Ar	37	3.7	8.5	8.7	9.4
Ar	50	3.6	15.6	16.8	26.7
Ar + 0.007% Methane #1	50	4.2	8.1	7.0	10.1
Ar + 0.007% Methane #2	50	4.2	9.4	8.9	10.9
Ar + 0.007% Methane #3	50	4.2	9.6	6.4	12.7
80% Ar + 20% Xe	50	2.5	15.7	14.2	16.4

Using data from Knoll (14:201), the limiting theoretical resolutions for argon can then be calculated for the three principal gamma rays of the external sources. Table VIII contains the data and the theoretical resolutions. The experimental values range from 2 to 3 times larger than the theoretical values for the  $^{241}\text{Am}$  and  $^{109}\text{Cd}$  and 3 to 4 times larger for the  $^{57}\text{Co}$ . The values for the  $^{57}\text{Co}$  were expected to be higher because the 122 keV peak included the 136 keV peak, since the resolution was not good enough to resolve it. The values at 50 Atm. are the highest, but the discharges in the detector began at a voltage of only 3600 volts. This was lower than the optimum voltage at 37 Atm. of 3700 volts.

Table VIII  
Limiting Theoretical Resolution

Source	Edep(keV)	F*	b*	W(eV)*	R(%)
$^{241}\text{Am}$	59.54	0.17	0.50	26.2	4.05
$^{109}\text{Cd}$	88.03	0.17	0.50	26.2	3.33
$^{57}\text{Co}$	122.01	0.17	0.50	26.2	2.83

\* These values (14:201) were assumed applicable at all pressures.

### Intrinsic Efficiency

The intrinsic efficiency of a detector is a measure of how many particles of a particular type and energy entering the detector are counted. It is defined as the number of net counts produced by a particular particle divided by the number of these particles entering the detector. For gamma rays, we can approximate the number of photons entering the detector by

$$N = f_g f_{tr} f_i A t_c \quad (6-5)$$

(Reference 11)

where  $f_g$  = the geometry factor

$f_{tr}$  = the transmission factor

$f_i$  = the branching ratio for the decay that produces the photons

$A$  = the activity of the source

$t_c$  = the collection time

Geometry Factor. The geometry factor for an external source can be approximated by the solid angle subtended by the detector. This is given by Knoll (14:95) as

$$f_g = .5 \{ 1 - d / (d^2 + r^2)^{0.5} \} \quad (6-6)$$

where  $d$  = the distance of the detector from the source

$r$  = radius of the circular detector surface

The actual detector source well and how it was modeled are depicted in Figure 13. Additionally, a source holder was used with some of the  $^{241}\text{Am}$  runs, which displaced the source an additional 0.75 inches. Table IX shows the calculated geometry factors.

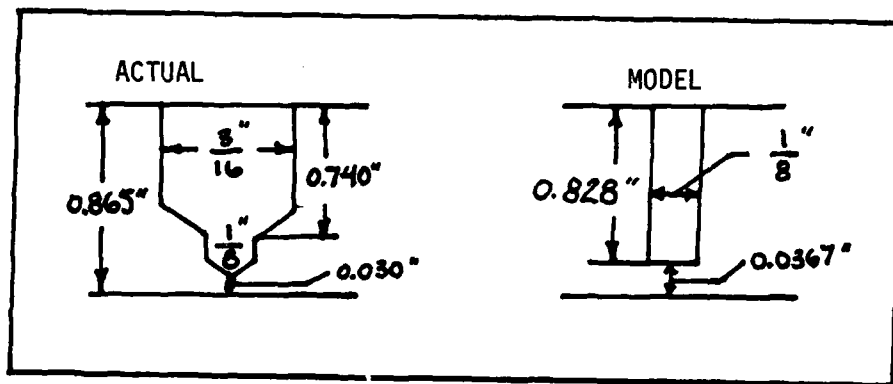


Figure 13. Actual Source Well and Model Used

Table IX  
Parameters for Calculating Geometry Factors

	Without Holder	With Holder
d	0.823" $\pm$ 0.1	1.573" $\pm$ 0.1
r	0.0625" $\pm$ 0.005	0.0625" $\pm$ 0.005
fg	0.00145 $\pm$ 0.00025	0.0004 $\pm$ 0.00003



Transmission Factors. The transmission factor for this experiment was assumed to be caused entirely by the absorption in the side of the detector case, i.e., the effects of the intervening air were neglected. The transmission factor is calculated using the following formula

$$f_{tr} = \text{Exp} (- \mu/\rho \rho x) \quad (6-7)$$

(Reference 12)

where  $\mu/\rho$  = the total mass absorption coefficient for iron

$\rho$  = the density of iron (7.86 gm/cm<sup>3</sup>)

$x$  = the thickness of the detector (from the model in Figure 13 it is approximately 0.0932 cm  $\pm$  0.03)

The calculated transmission factors are shown in Table X.

Table X  
Transmission Factors

Gamma Energy (keV)	$\mu/\rho$ (Reference 19)	ftr
59.54	1.174	0.4232 $\pm$ 0.117
88.01	0.4941	0.6963 $\pm$ 0.08
122.06	0.2896	0.8088 $\pm$ 0.06

Theoretical Efficiency. A theoretical calculation of the intrinsic efficiencies for a narrow beam can be made by calculating the fraction of photons which interact by the photoelectric effect within the detector. This is given by

$$\text{Eff}_T = \tau/\mu \{1 - \text{Exp}(- \mu/\rho \rho x)\} \quad (6-8)$$

where  $\tau$  = the photoelectric cross section for the gas  
 $\mu$  = the total absorption cross section for the gas  
 $\rho$  = the density of the gas  
 $x$  = the diameter of the detector (4.128 cm)

The factors used to calculate the theoretical efficiencies for argon are shown in Table XI.

Table XI  
Factors For Theoretical Efficiencies

Cross section (Ref 19)	Gamma Energies (keV)		
	59.54	88.01	122.03
$\tau/\rho$ (cm <sup>2</sup> /gm)	0.2625	0.1197	0.0307
$\mu/\rho$ (cm <sup>2</sup> /gm)	0.4488	0.2407	0.1723
Pressure (Atm.)	*Density (gm/cm <sup>3</sup> )		
20	0.0334		
30	0.0506		
37	0.0680		
50	0.0857		

\* These were calculated using Van der Waals relation.

Calculated Intrinsic Efficiencies. The intrinsic and theoretical efficiencies were calculated using the information in Tables IX, X, and XI for the spectra obtained at the optimum voltage setting previously described (see Table VII). The activities, collection times, and net counts are shown in Appendix E. The counts for the  $^{57}\text{Co}$  include the counts for the 136 keV gamma. The efficiencies are presented in Table XII.

The experimental efficiencies are all within one order of magnitude of the theoretical ones. Considering that there were no rigid source holders to fix the position and orientation of the sources, this is probably as good as can be expected. In addition, the efficiencies observed for  $^{241}\text{Am}$  and  $^{109}\text{Cd}$  gammas are lower than the theoretical while that of the  $^{57}\text{Co}$  gamma is higher (reflecting the addition of the 136 keV gammas). There was also an increase in the efficiencies by a factor of approximately 3.5 for all three energies at 50 atm. with the addition of 20% xenon.

Table XII  
Experimental And Theoretical Efficiencies

Gas Mixture	Energy (keV)	Efficiencies	
		Exp.	Theo.
20 Atm Ar	59.54	$0.006 \pm .002$	0.035
	88.01	$0.003 \pm .0007$	0.016
	122.03	$0.006 \pm .001$	0.004
30 Atm Ar	59.54	$0.029 \pm .009$	0.052
	88.01	$0.006 \pm .002$	0.024
	122.03	$0.012 \pm .003$	0.006
37 Atm Ar	59.54	$0.025 \pm .007$	0.069
	88.01	$0.014 \pm .003$	0.032
	122.03	$0.011 \pm .003$	0.008
50 Atm Ar	59.54	$0.032 \pm .010$	0.086
	88.01	$0.016 \pm .004$	0.041
	122.03	$0.012 \pm .003$	0.011
50 Atm Ar + .007% Methane (Run1)	59.54	$0.038 \pm .012$	not calculated
	88.01	$0.013 \pm .003$	"
	122.03	$0.015 \pm .003$	"
50 Atm Ar + .007% Methane (Run2)	59.54	$0.034 \pm .010$	"
	88.01	$0.015 \pm .004$	"
	122.03	$0.014 \pm .003$	"
50 Atm Ar + .007% Methane (Run3)	59.54	$0.036 \pm .011$	"
	88.01	$0.013 \pm .003$	"
	122.03	$0.014 \pm .003$	"
50 Atm 80% Ar + 20% Xe	59.54	$0.119 \pm .040$	"
	88.01	$0.039 \pm .009$	"
	122.03	$0.049 \pm .010$	"

## VII. Conclusions And Recommendations

### Conclusions

The purpose of this study was to build, test, and evaluate a high pressure proportional detector for use in the analysis of radioactive noble gases.

Based on the experimental data, this system in its present configuration is not suitable for this analysis. The present design of the field tube inside the detection chamber produces end effects that would have made any data collected with an internal source, i.e., using the entire length of the anode, completely unusable. In addition, the purification process was not adequate to purify the available xenon gas (99.9% pure) enough to produce adequate spectra. Consequently, no data collection with a radioactive noble gas source was attempted.

The results with the external sources over the center of the anode (a region absent from the end effects) indicate that the system has some potential to do this analysis if modified to eliminate the end effects. The results using ultra pure argon that was unpurified produced resolutions two to three times worse than those predicted by theory. The operation at 50 Atm. was limited, though, because there was a large electrical discharge in the detector at a fairly low voltage (3600 volts as opposed to 3800 volts at 37 Atm.). A mixture of argon with 0.007% methane at 50 Atm. eliminated the discharge problem and produced spectra at 4200 volts with a resolution in the range of two times worse than the theoretical resolution predicted (see Table VIII) for argon at 50 Atm. Although other mixtures with greater amounts of methane were attempted,

the spectra produced were not usable because of a Compton type interaction that produced a broad tail on the photopeak.

The 80% argon and 20% xenon mixture at 50 Atm. produced mixed results. This gas mixture, as predicted by the non-metastable Penning process, has a much higher gas multiplication (optimum operating voltage was 2500 volts as opposed to 4200 volts for the argon-methane mixture). This has the advantage of less discharge inside the detector and, consequently, a longer anode life. Although with this configuration changing, the anode wire is a fairly simple process; everytime the chamber is opened, there is a potential of contamination. The disadvantage of this mixture is that the resolution was almost double that of the argon-methane mixture. This was possibly caused by the impurity level in the xenon as discussed previously.

Finally, the system has two inherent problems that will seriously limit its value as a production system. First, the purification and pressurization cycle require approximately 12 hours to complete. That would limit the number of samples analyzed to, at the very best, two per day. The second problem is that the sensitive volume of the detector only occupies 37% of the total volume of the detector. With the anticipated low volume and low activity Xe samples, the accuracy of the analysis would be less than optimum.

#### Recommendations

It is recommended that the study of this system's potential to analyze radioactive noble gases be continued. Prior to any additional work, the detector will have to be modified to eliminate the end effects. This could be accomplished by installing larger diameter field tubes and applying the appropriate potential (as discussed in Chapter

III) to eliminate the end effects. These field tubes should be epoxied in place on the ceramic end pieces of the center section. Electrical contact will have to be made through the side of the detector. This can be accomplished by soldering a narrow rod to the field tube with a spring contact on top. When the center section is installed in the detector, this rod would make electrical contact with the isolate cable in the side of the detector. Figure 14 shows a possible configuration for the right hand connection. The left hand side would be configured in the same fashion. A locating pin would also have to be installed in the center section to ensure correct alignment.

The second recommendation is to develop a method to measure quantitatively the level of impurities in the fill gas so that the operation of the purification system can be studied. Presently there is no way to judge its effectiveness other than by qualitative observations. While investigating the purification process, the calcium turnings should be replaced with a mixture of Zr-Ti turnings, the same as Lackey used (17:61) to see if it proves to be more effective. In addition, since the results were reasonable with the unpurified ultra high purity argon, recommend the highest purity xenon available be obtained. Xenon with the same level of impurities as the ultra pure argon might produce useful results with no purification.

Finally, a mixture of argon and xenon should be investigated as potential fill gases for the radioactive noble gas samples. These would have the advantages of using some inexpensive argon in place of the xenon, as well as lower operating voltages. The efficiency would obviously not be as high as with pure xenon, but some combination may provide a useful mixture with an acceptable tradeoff.

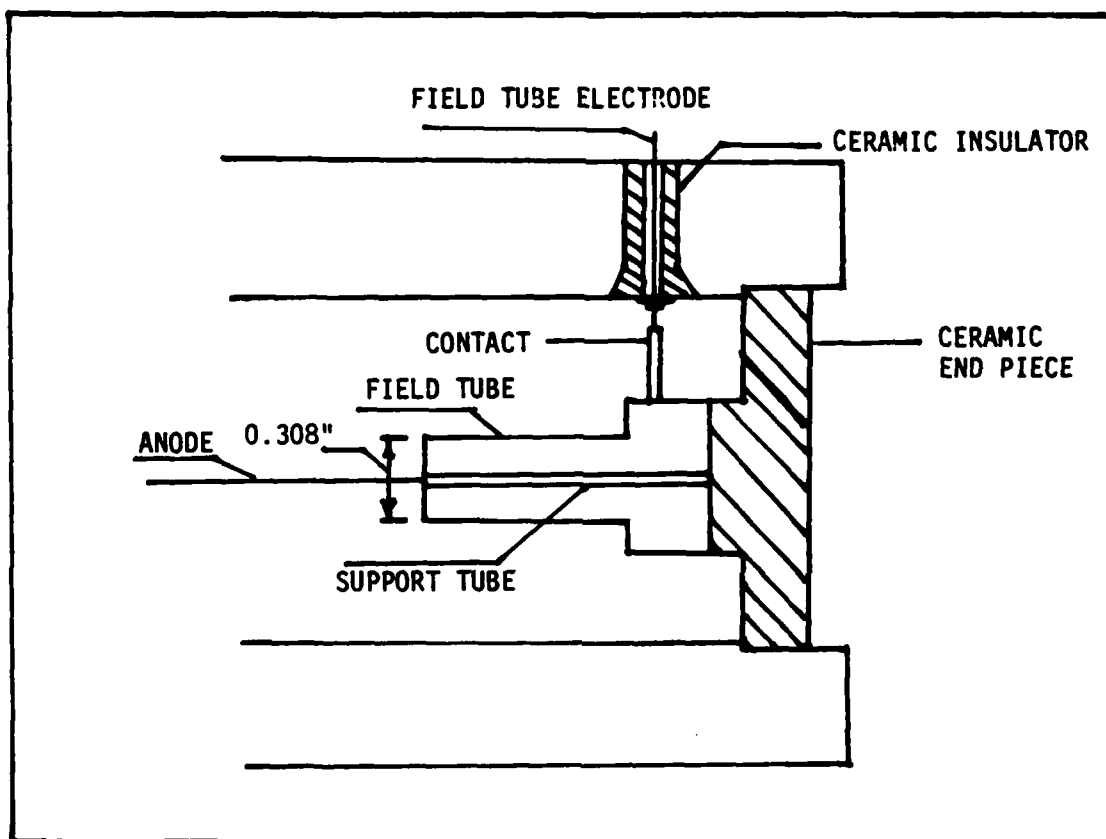


Figure 14. Field Tube Configuration



Appendix A  
Equipment Calibration

Volume Measurement

The critical volumes of the gas-handling system were measured by expanding a known volume of Argon ( $1058.28 \text{ cm}^3 \pm 0.20 \text{ cm}^3$ ) at 1 atm. into an initial volume (between valves 5 and 7). Then subsequent expansions of this gas into other sections of the detection system were made. Pressure was measured after each expansion using a Wallace and Tiernan gauge (model FA145). The volumes were then calculated using the ideal gas law. Table XIII lists the measured volumes for the sections of the gas-handling system.

Table XIII. Volumes in Detection System

Volume Between Valve Numbers	Name	Volume (cm3)	Uncertainty (cm3)
#4, #5, #6	"T" section	44.89	$\pm 0.95$
#6	detector	257.60	$\pm 1.2$
#1, #2, #3, #4	reservoir	29051.0	$\pm 171.5$

Pressure Gauge

The Wallace and Tiernan gauge was also used to calibrate the system pressure gauge. The system was filled to various pressures and readings were made off both gauges. The procedure was followed for both the high and low scale of the pressure gauge. The data was plotted and the following least squares fits were obtained.

#### High Scale

$$P(\text{actual}) = 1.00475 \times P(\text{system}) - 0.281472$$

$$\text{slope} \pm 0.00289$$

$$\text{intercept} \pm 0.1325$$

#### Low Scale

$$P(\text{actual}) = 0.98222 \times P(\text{system}) - 0.03057$$

$$\text{slope} \pm 0.00102$$

$$\text{intercept} \pm 0.1045$$

#### MCA

The channel scale of the MCA was calibrated by introducing varying voltages from a precision pulser directly into the MCA, and then measuring the channel number of the pulse. The input pulses were measured on an oscilloscope and graduated up to 6000 mV. The data was plotted in two segments, below channel 111 and above channel 111 (1000 mV). The following least squares fits were obtained.

#### Low End Calibration

$$\text{ph(mV)} = \text{CH\#} \times 8.913 \text{ (mV/CH)} + 8.1420 \text{ (mV)}$$

$$\text{slope} \pm 0.071$$

$$\text{intercept} \pm 3.996$$

#### High End Calibration

$$\text{ph(mV)} = \text{CH\#} \times 8.572 \text{ (mV/CH)} + 55.45 \text{ (mV)}$$

$$\text{slope} \pm 0.0534$$

$$\text{intercept} \pm 33.25$$

### Linear Amplifier

The Linear Amp (LA) was calibrated by introducing a voltage from a precision pulser directly into the input of the LA and measuring both the input and output signals on an oscilloscope. The data was fit with a least squares fit. The slope is the gain of the LA.

with gain set at 10

$$G_{LA} = 8.60 \pm 0.02$$

with Gain set at 25

$$G_{LA} = 21.00 \pm 0.08$$

### Preamplifier

To calibrate the preamplifier (in the x 10 setting), a proportional flow detector was used with an  $^{241}\text{Am}$  source placed inside the cylinder. The 5.49 MeV alpha peak was used to measure the energy deposited, with the detector operated in the ionization region. The peak was measured in channel 67 $\pm$ 1 on the MCA. Using the results of the MCA calibration

$$ph = 605.313 \text{ (mV)} \pm 10.2$$

Then using Eq. 6-1

$$ph = Q M G_{PA} G_{LA}$$

$$\text{the gain } G_{PA} = ph / (Q G_{LA} M)$$

where

$$Q = E_{\text{dep}}/W \text{ e}$$

$$E_{\text{dep}} = 5.49 \text{ (MeV)}$$

$$W = 26.3 \text{ (eV)}$$

$$G_{\text{LA}} = 8.6 \pm 0.02$$

$$M = 1$$

Then  $G_{\text{PA}} = 2107.4 \text{ (mV/pC)} \pm 35.5$

## Appendix B

### The External Sources

The external gamma sources used were  $^{241}\text{Am}$ ,  $^{109}\text{Cd}$ , and  $^{57}\text{Co}$ .  $^{241}\text{Am}$  decays by an alpha emission to  $^{237}\text{Np}$ . Approximately 86% of these decays leave the  $^{237}\text{Np}$  in an excited state 59.54 keV above its ground state (18:430). The  $^{109}\text{Cd}$  decays by a gamma with an energy of 88.03 keV and a branching ratio of 0.0361 (18:250). The  $^{57}\text{Co}$  emits two gamma rays. One is 122.01 keV with a branching ratio of 0.856, and the other is 136.3 keV with a branching ratio of 0.106 (18:191). With so many more of the 122.01 keV gammas emitted, it was assumed that the  $^{57}\text{Co}$  peak was at 122.01 keV. There are other photons emitted by these sources, but they either do not penetrate the case or pass right through it. Table XIV contains the source activity data.

Table XIV  
Source Information

Ident.	Source	Activity	Date	Uncertainty
A	$^{241}\text{Am}$	10 mCi	10 Mar 74	$\pm 10\%$
B	$^{109}\text{Cd}$	65 uCi	7 Nov 83	$\pm 10\%$
C	$^{57}\text{Co}$	97 uCi	9 Apr 84	$\pm 10\%$
D	$^{241}\text{Am}$	300 uCi	10 Dec 71	$\pm 10\%$
E	$^{57}\text{Co}$	17.9 uCi	9 Apr 84	$\pm 10\%$

Appendix C  
Sample Spectra

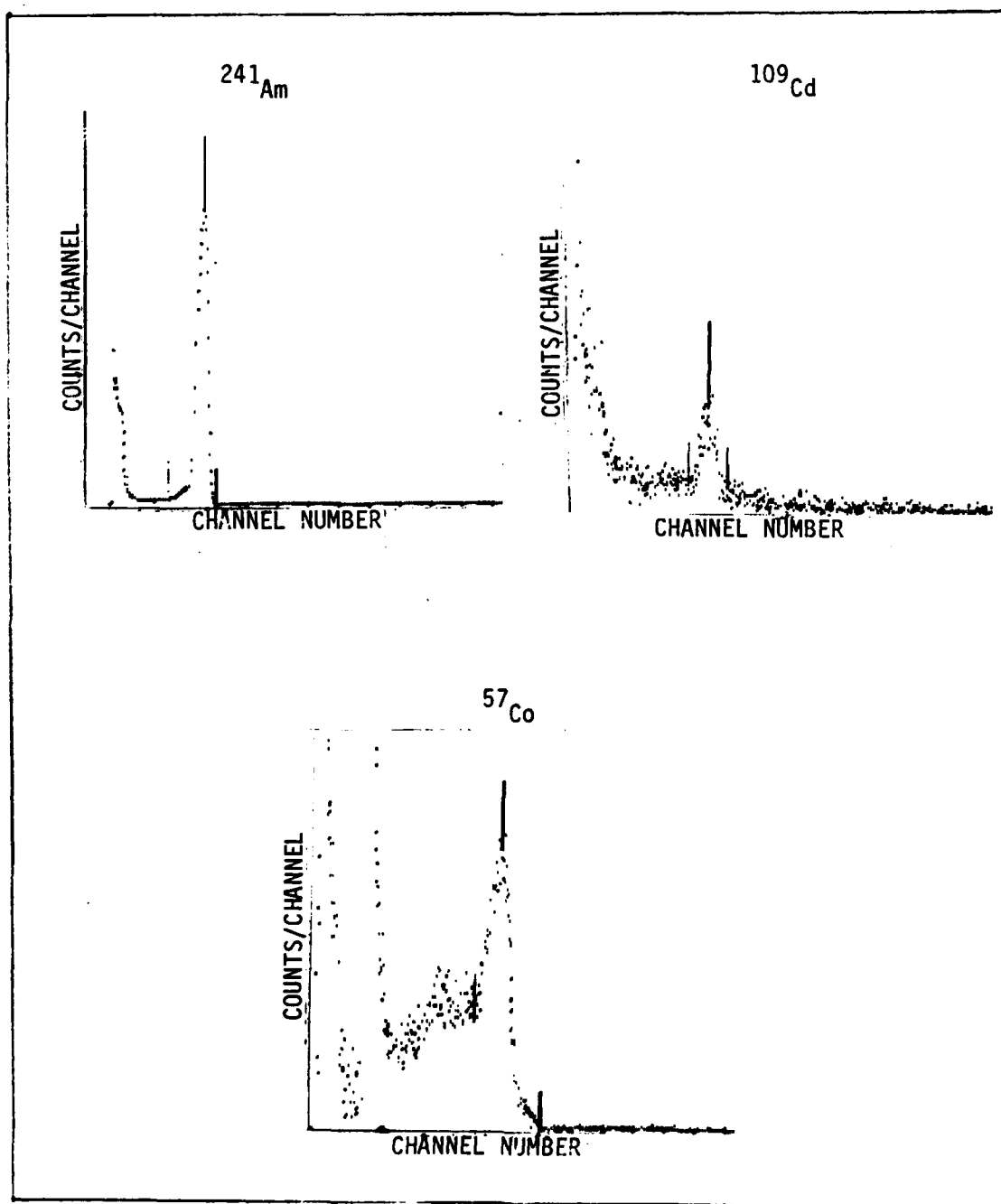


Figure 15. Argon At 20 Atm And 2600 Volts

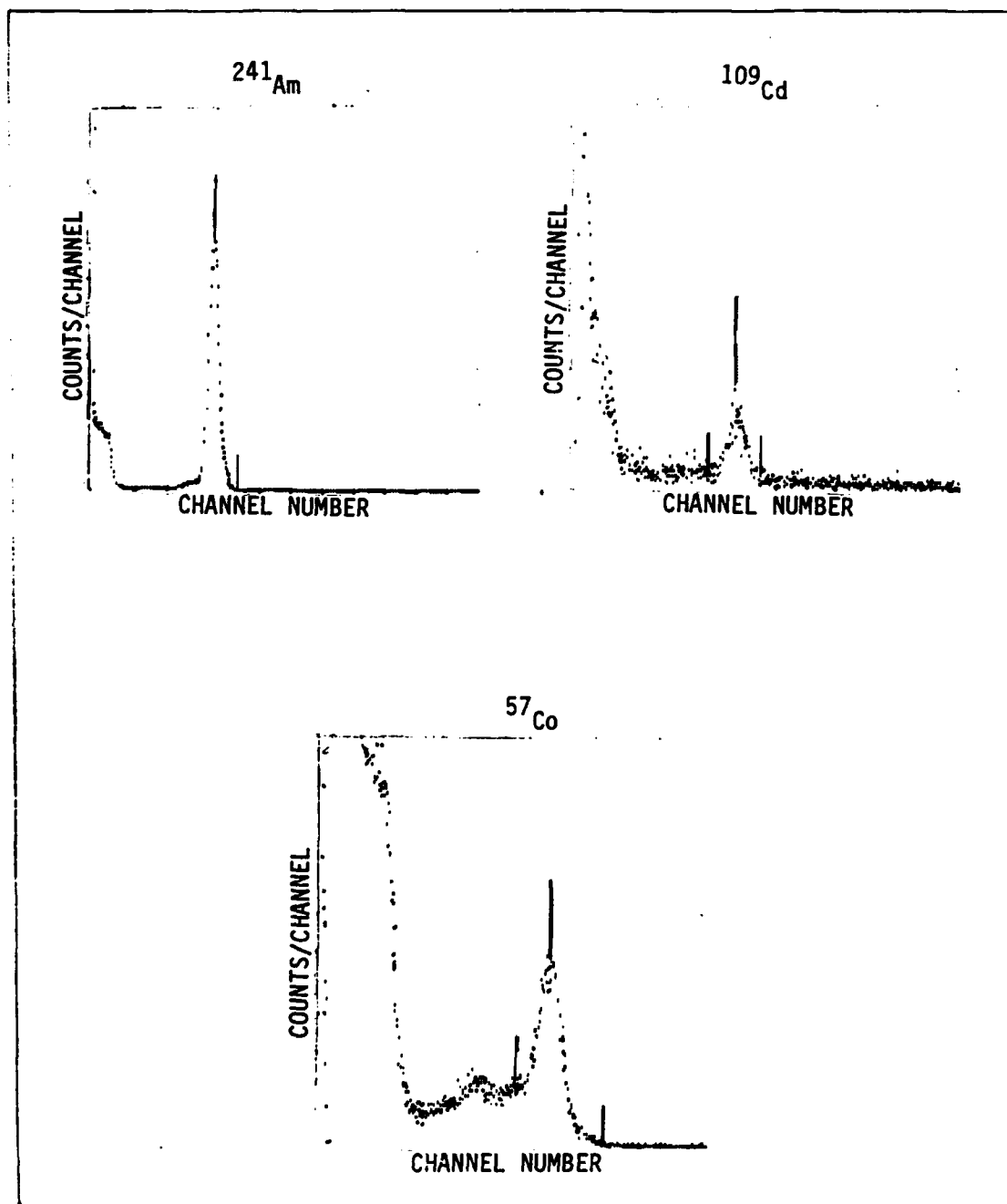


Figure 16. Argon At 30 Atm And 3300 Volts

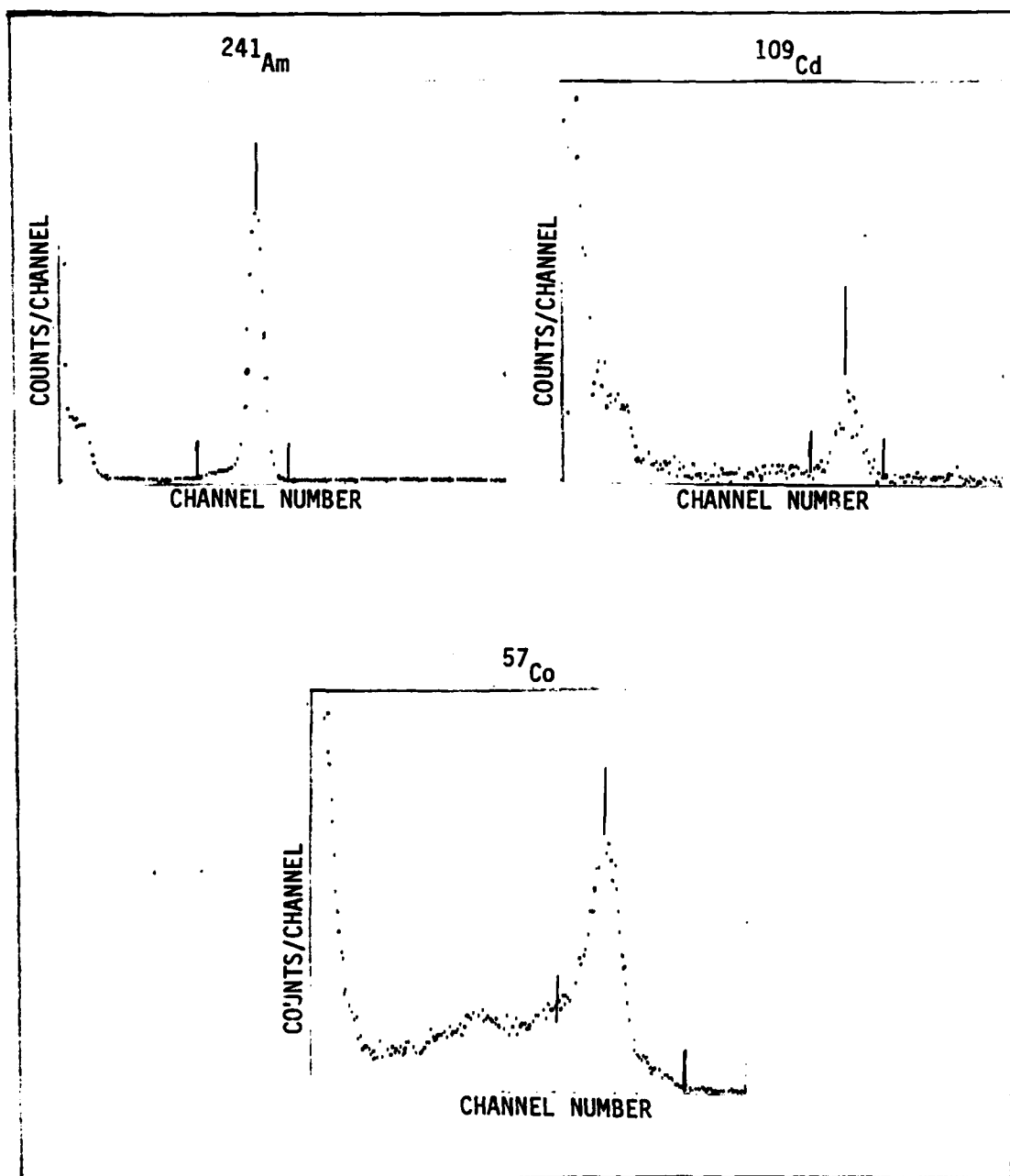


Figure 17. Argon At 37 Atm And 3500 Volts



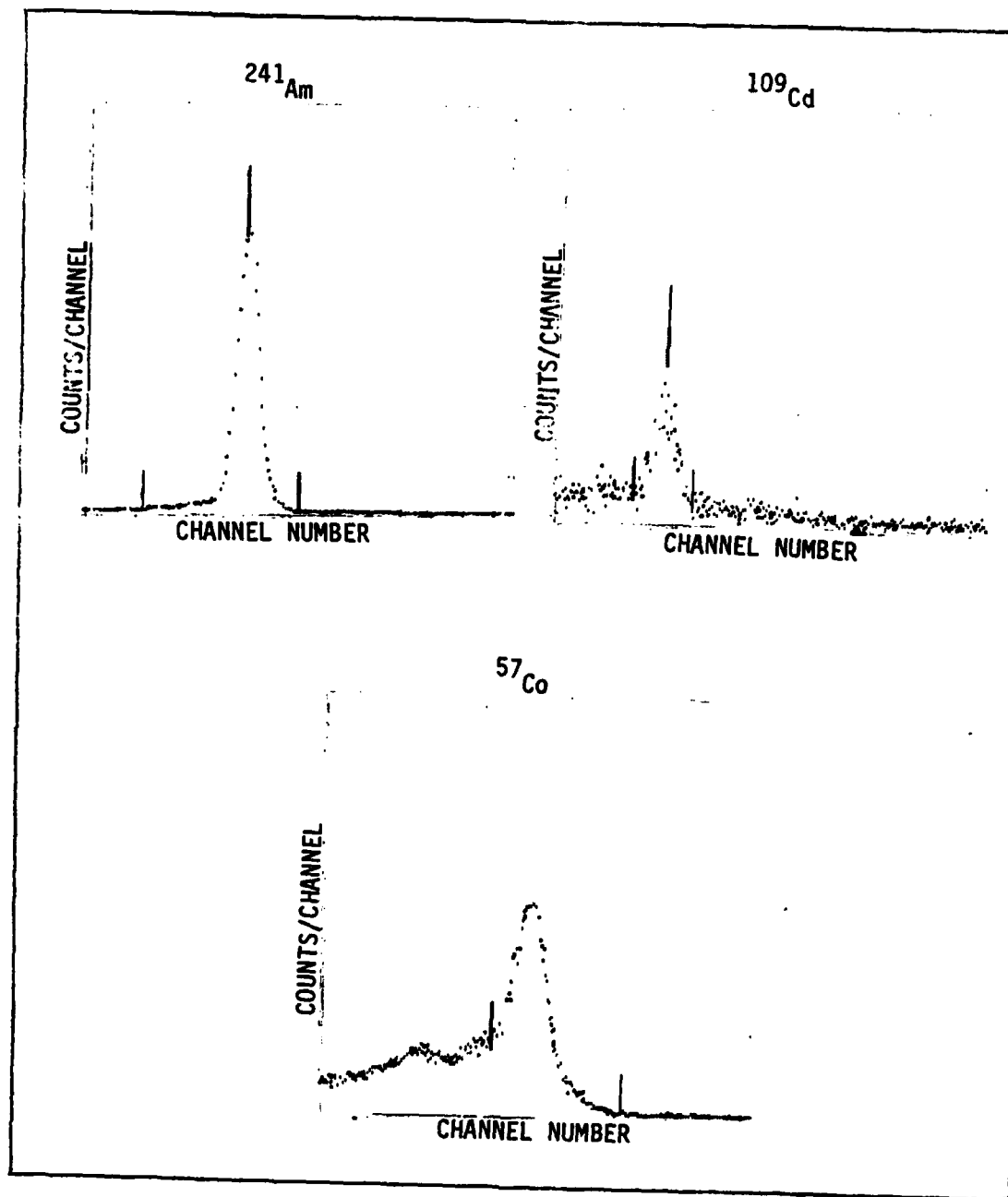


Figure 18. Argon With 0.007% Methane At 50 Atm And 4100 Volts

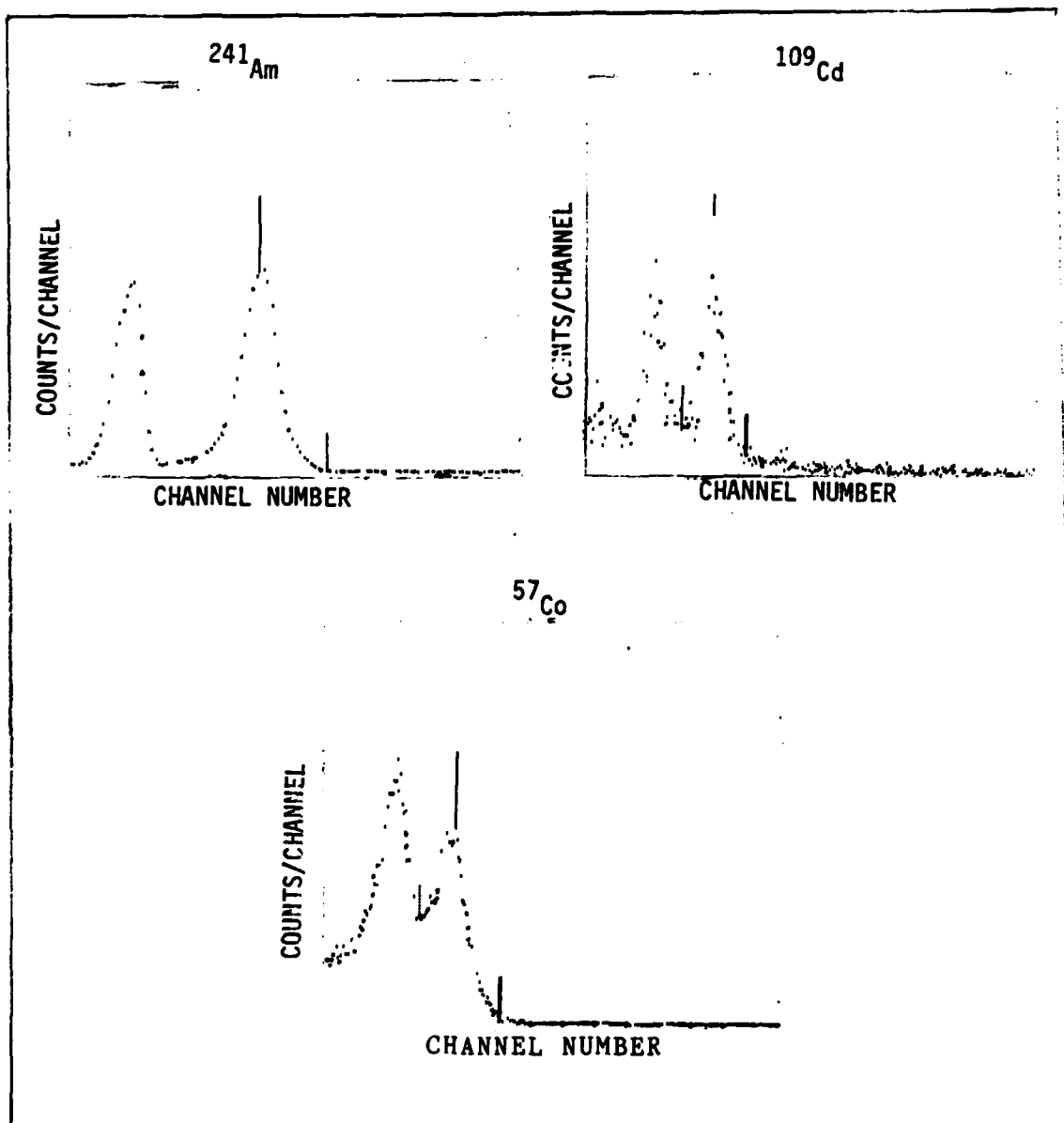


Figure 19. 80% Argon And 20% Xenon At 50 Atm And 2500 Volts

Appendix D  
Resolution Versus Voltage Plots

## RESOLUTION vs. VOLTAGE

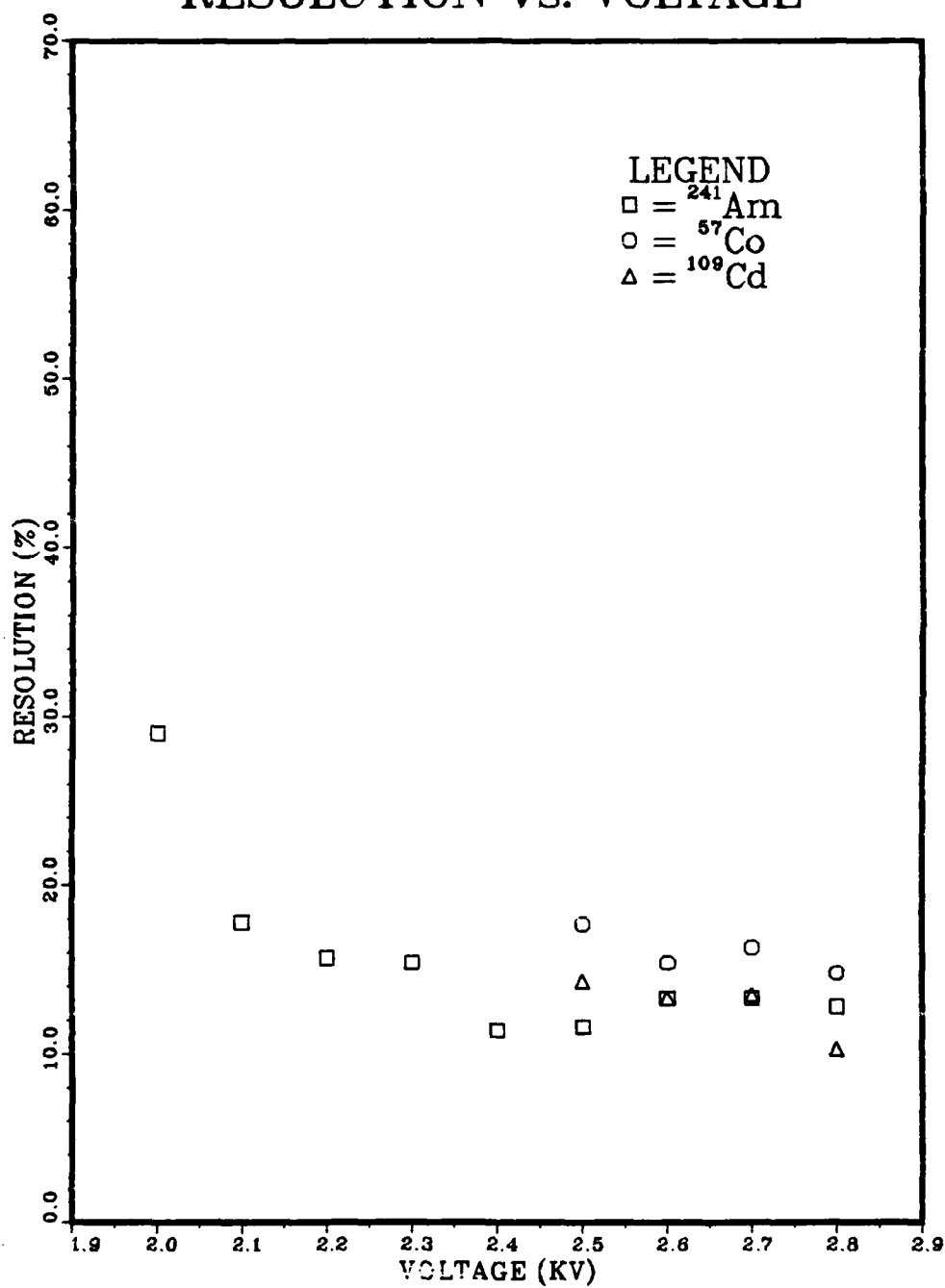


Figure 20. Resolution Vs. Anode Voltage (Argon At 20 Atm)

## RESOLUTION vs. VOLTAGE

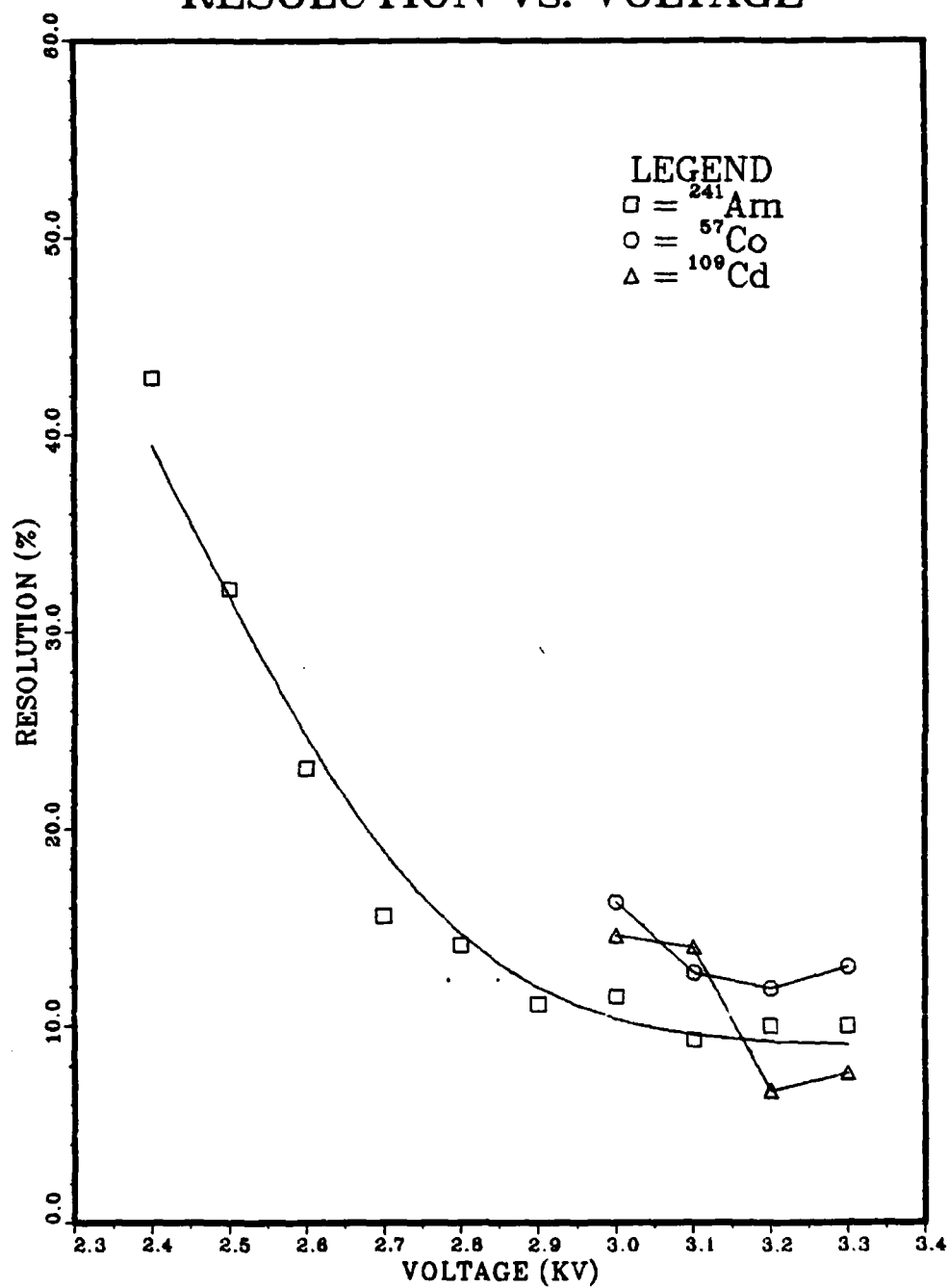


Figure 21. Resolution Vs. Anode Voltage (Argon At 30 Atm)

## RESOLUTION vs. VOLTAGE

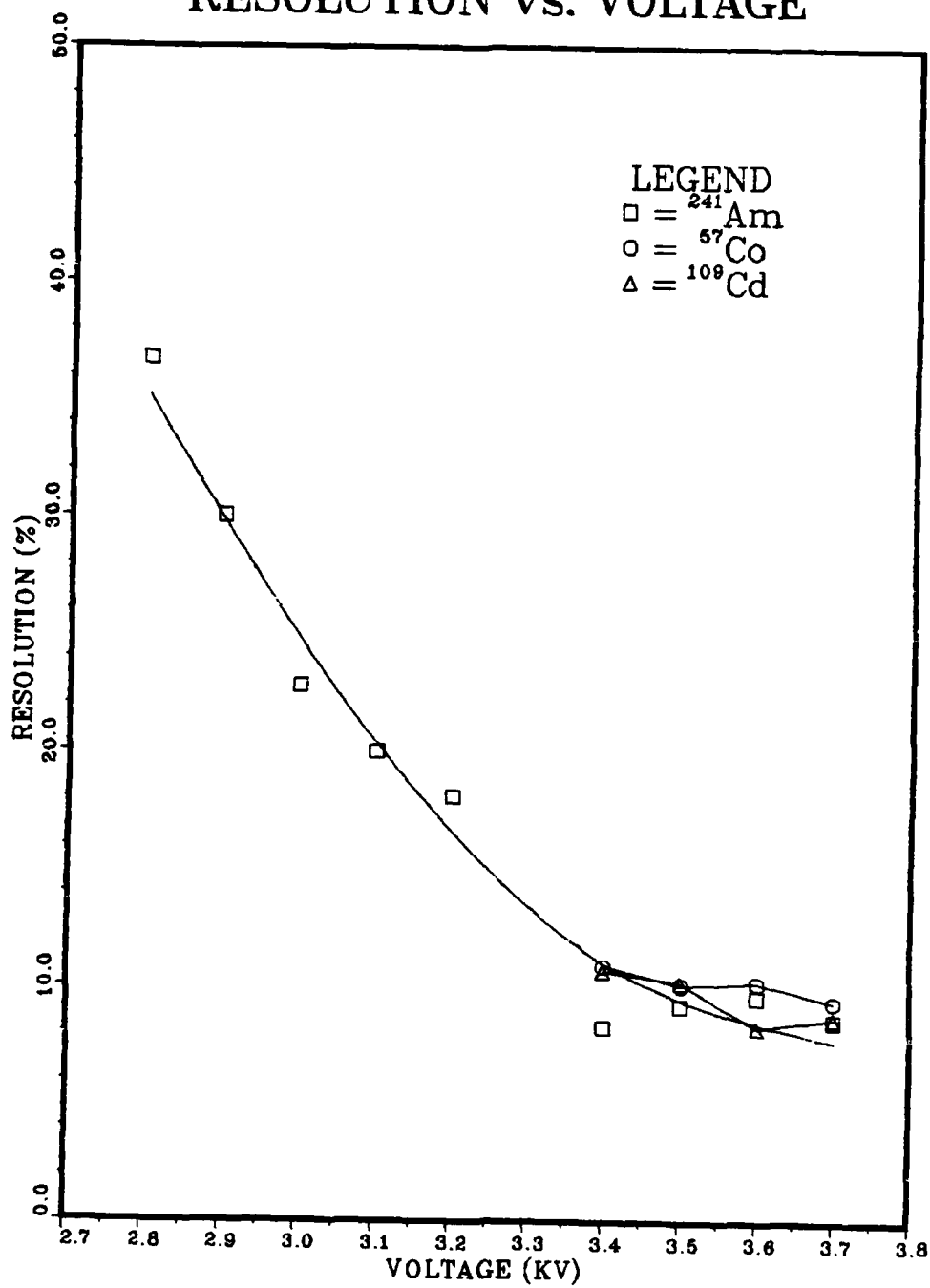


Figure 22. Resolution Vs. Anode Voltage (Argon At 37 Atm)

## RESOLUTION vs. VOLTAGE

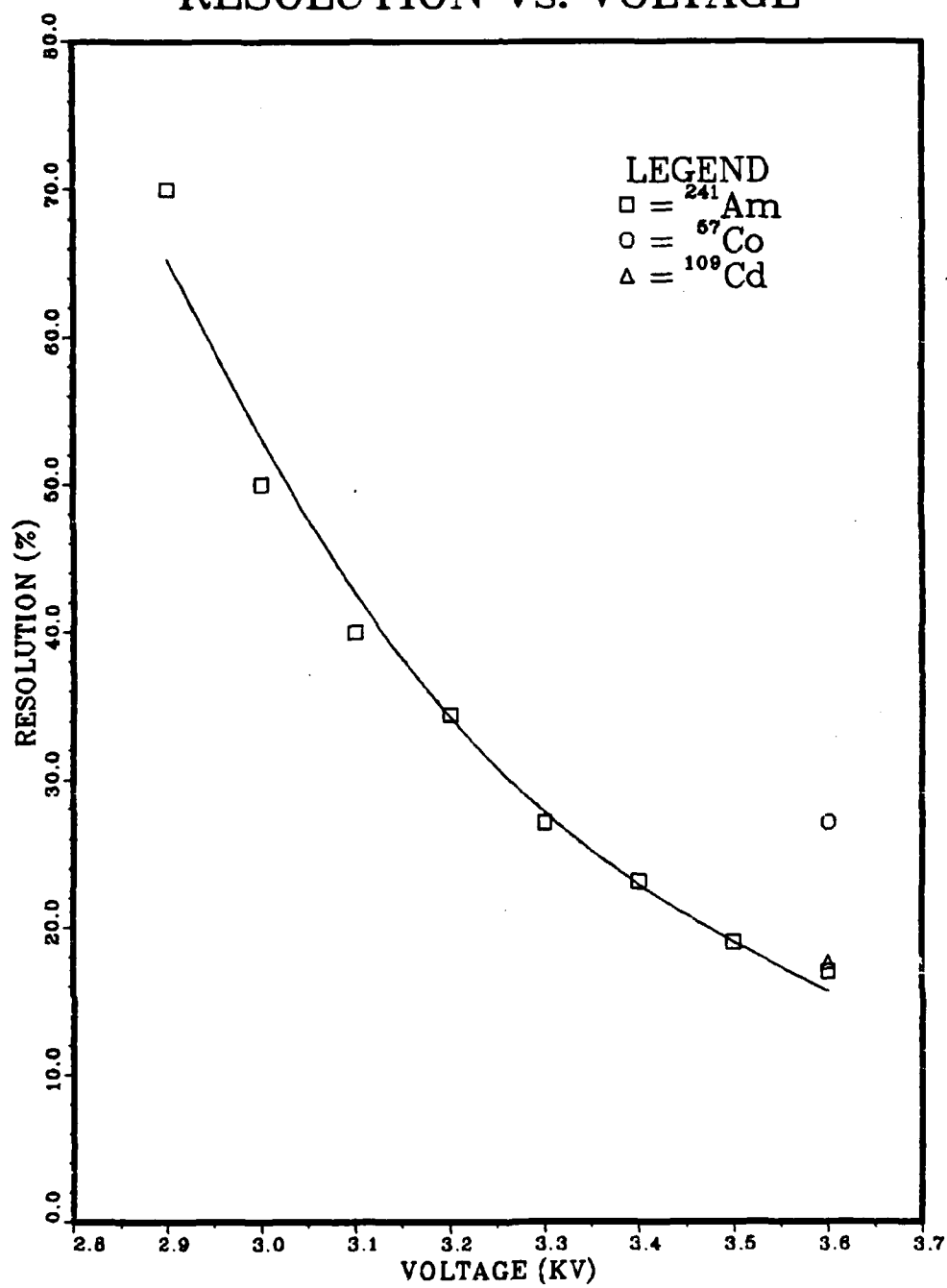


Figure 23. Resolution Vs. Anode Voltage (Argon At 50 Atm)

## RESOLUTION vs. VOLTAGE

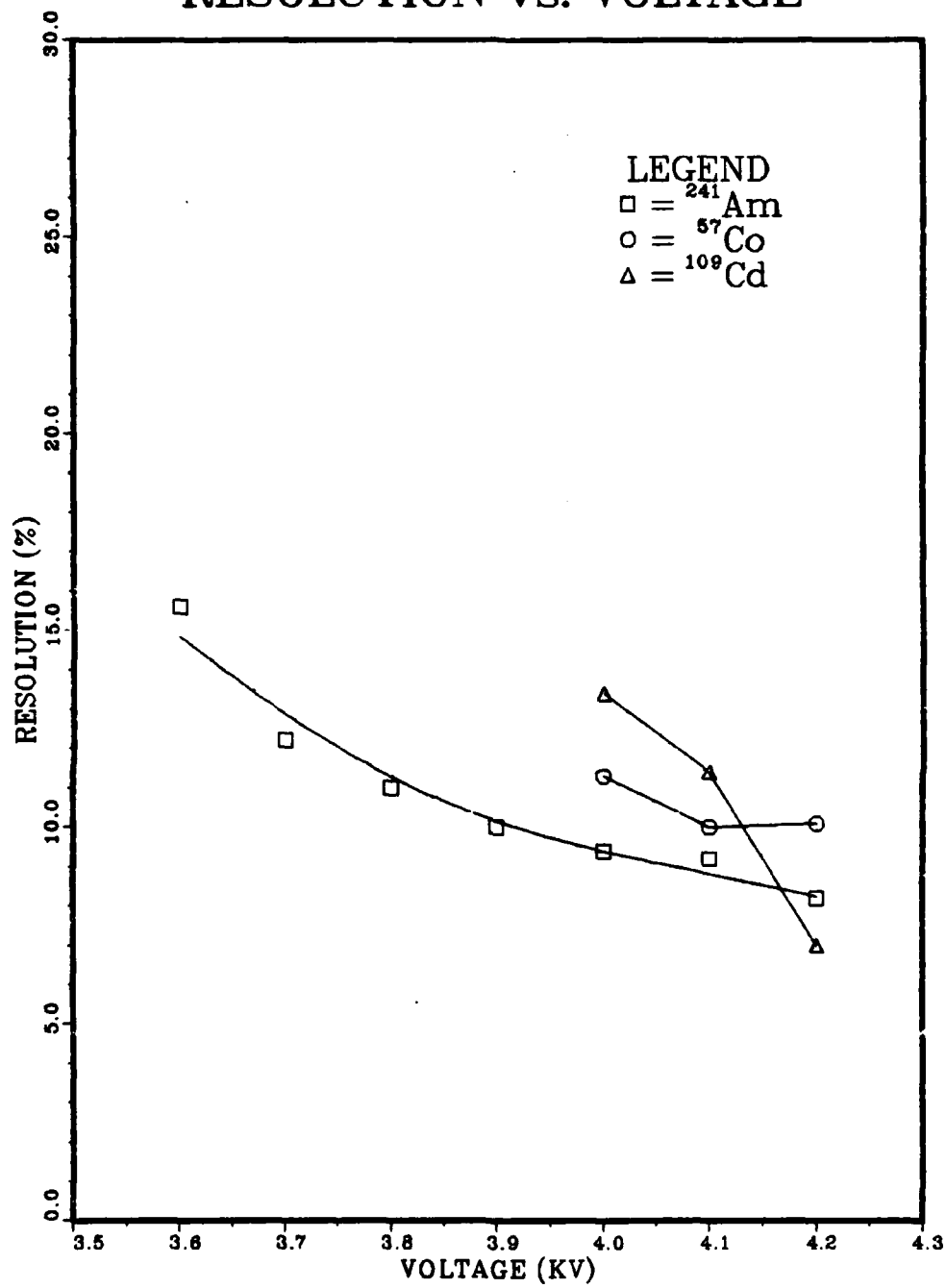


Figure 24. Resolution Vs. Anode Voltage (Argon +.007% Methane At 50 Atm)

## RESOLUTION vs. VOLTAGE

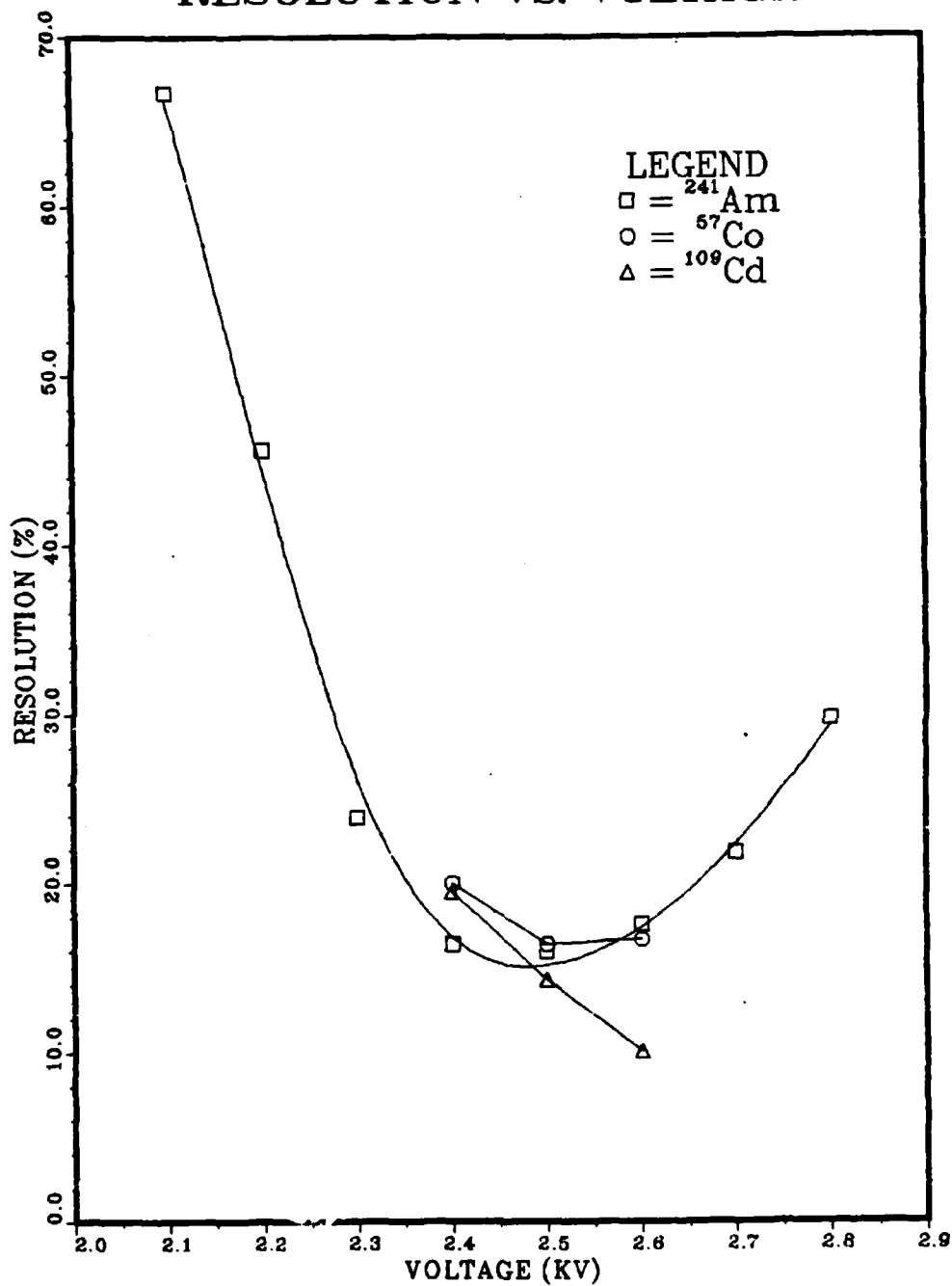


Figure 25. Resolution Vs. Anode Voltage (80% Argon + 20% Xenon At 50 Atm)



# Appendix E

## Factors Used To Calculate Intrinsic Efficiencies

Gas	Atm.	Volt.	Source	Act.(dis/sec)	tc(sec)	Count
Ar	20	2800	A	3.643E+8	400	188764
		2800	B	1.400E+6	2000	287
		2800	C	2.095E+6	400	5411
Ar	30	3200	A*	3.643E+8	400	254169
		3200	B	1.344E+6	400	120
		3200	C	1.946E+6	400	9449
Ar	37	3700	A*	3.643E+8	400	215311
		3700	B	1.385E+6	1000	708
		3700	C	2.048E+6	400	9262
Ar	50	3600	A*	3.643E+8	400	280159
		3600	B	1.377E+6	1000	821
		3600	C	2.027E+6	400	10079
Ar	50	4200	A*	3.643E+8	400	337445
.007%		4200	B	1.359E+6	1000	644
Methane		4200	C	1.981E+6	400	12124
Ar	50	4200	A*	3.643E+8	400	299508
.007%		4200	B	1.357E+6	1000	757
Methane		4200	C	1.967E+6	400	10852
Ar	50	4200	A*	3.643E+8	400	317299
.007%		4200	B	1.350E+6	1000	657
Methane		4200	C	1.961E+6	400	11213
Ar	50	2500	D	1.087E+7	400	112795
+		2500	B	1.342E+6	400	761
Xe		2500	E	358209	400	7114

\* indicates sources used with the additional .75" source holder.

Sources are identified by letter in Appendix B.

## Bibliography

1. Andrews, Wayne L. Evaluation of A Detection System Employing Two Semiconductors for Analysis of Radioactive Noble Gases. Unpublished thesis. Wright-Patterson Air Force Base, Ohio; Air Force Institute of Technology, March 1982.
2. Bambynek, W. "On Selected Problems in the Field of Proportional Counters," Nuclear Instruments & Methods, 112: 103-110 (1973).
3. Berrgren, Stephen R. A Cryogenic Xenon Ionization Chamber Detector for the Analysis of Radioactive Noble Gases. Unpublished thesis. Wright-Patterson Air Force Base, Ohio; Air Force Institute of Technology, March 1983.
4. Charles, M. W. "Gas Gain Measurements in Proportional Counters," Journal of Physics E: Scientific Instruments, 5: 219-234 (1968).
5. Chitwood, R. B. "Production of Noble Gases by Nuclear Fission," page 76 in Proceedings of the Noble Gas Symposium, ERDA CONF-730915, Stanley, R. E. and Moghissi, A., Editors, 1974.
6. Cockroft, A. L. and S. C. Curran. "The Elimination of the End Effects in Counters," The Review of Scientific Instruments, 22: 37-42 (January 1951).
7. Fano, V. "Ionization Yield of Radiations. II. The Fluctuation of the Number of Ions," Physical Review, 72: 26-29 (July 1947).
8. Gibbons, M. R. Evaluation of a Gridded Ionization Chamber for the Detection of Noble Gases. Unpublished thesis. Wright-Patterson Air Force Base, Ohio; Air Force Institute of Technology, March 1984.
9. Gibbs, D. S. et al. "Purification of the Rare Gases," Industrial and Engineering Chemistry, 48: 289-296 (1956).
10. Gruhn, C. R. and R. Loveman. "A Review of the Physical Properties of Liquid Ionization Chamber Media," IEEE Transactions on Nuclear Science, NS-26 (1); 110-119 (February 1979).
11. Hunt, K. K. Analysis of A Semiconductor Detection System for Measuring Radioactive Noble Gases. Unpublished thesis. Wright-Patterson Air Force Base, Ohio; Air Force Institute of Technology, December 1976.
12. John, G. Unpublished class notes on Nuclear Physics (NE 6.51); Air Force Institute of Technology, Wright-Patterson Air Force Base, Ohio, 1984.

13. Knapp, J. J. Study of the Characteristics of High Pressure Proportional Counters for the Detection of Radioactive Noble Gases. Unpublished thesis. Wright-Patterson Air Force Base, Ohio; Air Force Institute of Technology, March 1983.
14. Knoll, Glenn F. Radiation Detection and Measurement. New York: John Wiley and Sons, 1979.
15. Kocher, D. C. Radioactive Decay Data Tables. Technical Information Center, U.S. Department of Energy, 1981.
16. Kubota, S. "NonMetastable Planning Effect in the Alpha Particle Ionization of Inert Gas Mixtures." Journal of the Physical Society of Japan. Vol. 29 1017-1029 (October 1970).
17. Lackey, R. E. Evaluation of A High Pressure Proportional Counter for the Detection of Radioactive Noble Gases. Unpublished thesis. Wright-Patterson Air Force Base, Ohio; Air Force Institute of Technology, March 1984.
18. Lederer, C. M., et al. Table of Isotopes (Seventh Edition). New York: John Wiley & Sons, 1978.
19. McMaster, W. H., et al. Compilation of X-ray Cross Sections. UCRL50174 Sec. II, Rev. 1. Livermore: Lawrence Radiation Laboratory, University of California, 1969.
20. Meek, M. E. and B. F. Rider. "Compilation of Fission Product Yields," Vallecitos B4Nuclear Center, ORNL TM-3515, August 1971.
21. Povinec, Pavel. "A Study of Proportional Counter Optimization for Long Term Counting," Nuclear Instruments and Methods, 163: 363368 (1979).
22. Rose, M. E. and S. A. Korff. "An Investigation of the Properties of Proportional Counters," Physical Review. Vol. 41: 850:859 (June 1947).
23. Rowe, Charles E. Quantitative Analysis of Radioactive Noble Gases With A SiLi Detector. Unpublished thesis. Wright-Patterson Air Force Base, Ohio: Air Force Institute of Technology, March 1974.
24. Sipila, H. "Inert Gas Mixtures for Proportional Counters," Nuclear Instruments and Methods. 133:251-252 (1976).
25. Williams, A. and R. I. Sara. "Parameters Affecting the Resolution of A Proportional Counter," International Journal of Applied Radiation and Isotopes, Vol. 13 229-238 (1962).

### Vita

William Lucyshyn was born in New York City, New York, on February 6, 1950. After graduating from Brooklyn Technical High School in 1967, he attended York College. He graduated from Richmond College with a Bachelor of Science Degree in Engineering Science in 1971. Entering the Air Force in 1972, he was commissioned a lieutenant through the OTS program. His initial assignment was to undergraduate navigator training at Mather AFB, Sacramento, California. Upon completion, he performed crew duties in a tactical airlift and two special operations squadrons. These were followed by a staff tour in the Special Plans Division, Headquarters, United States Air Forces Europe. After departing Germany, he was assigned to the Air Force Institute of Technology in 1983.

Permanent address: 86-19 102 Street  
Richmond Hill, New York  
11418

UNCLASSIFIED

SECURITY CLASSIFICATION OF THIS PAGE

## REPORT DOCUMENTATION PAGE

1a. REPORT SECURITY CLASSIFICATION UNCLASSIFIED			1b. RESTRICTIVE MARKINGS None		
2a. SECURITY CLASSIFICATION AUTHORITY N/A			3. DISTRIBUTION/AVAILABILITY OF REPORT Distribution Unlimited  UNCLASSIFIED		
2b. DECLASSIFICATION/DOWNGRADING SCHEDULE N/A					
4. PERFORMING ORGANIZATION REPORT NUMBER(S) AFIT/GNE/PH/85M-15			5. MONITORING ORGANIZATION REPORT NUMBER(S)		
6a. NAME OF PERFORMING ORGANIZATION Air Force Institute of Technology		6b. OFFICE SYMBOL (If applicable) EN	7a. NAME OF MONITORING ORGANIZATION		
6c. ADDRESS (City, State and ZIP Code) Wright-Patterson Air Force Base, OH 45433			7b. ADDRESS (City, State and ZIP Code)		
8a. NAME OF FUNDING/SPONSORING ORGANIZATION		8b. OFFICE SYMBOL (If applicable)	9. PROCUREMENT INSTRUMENT IDENTIFICATION NUMBER		
8c. ADDRESS (City, State and ZIP Code)			10. SOURCE OF FUNDING NOS.		
			PROGRAM ELEMENT NO.	PROJECT NO.	TASK NO.
11. TITLE (Include Security Classification)					
12. PERSONAL AUTHOR(S) Lucyshyn, William					
13a. TYPE OF REPORT Final		13b. TIME COVERED FROM _____ TO _____		14. DATE OF REPORT (Yr., Mo., Day) 10 Mar 85	
15. PAGE COUNT 86					
16. SUPPLEMENTARY NOTATION					
17. COSATI CODES			18. SUBJECT TERMS (Continue on reverse if necessary and identify by block number)		
FIELD	GROUP	SUB. GR.	Radioactive      Noble gas		
			Xenon              Proportional counter		
			High pressure		
19. ABSTRACT (Continue on reverse if necessary and identify by block number)					
Title: EVALUATION OF A HIGH PRESSURE PROPORTIONAL COUNTER FOR THE DETECTION OF RADIOACTIVE NOBLE GASES					
Approved for public release: 1AW AFR 190-17. E. E. WOLVER Dean for Research and Professional Development Air Force Institute of Technology (ATC) Wright-Patterson AFB OH 45433					
20. DISTRIBUTION/AVAILABILITY OF ABSTRACT UNCLASSIFIED/UNLIMITED <input checked="" type="checkbox"/> SAME AS RPT. <input type="checkbox"/> DTIC USERS <input type="checkbox"/>			21. ABSTRACT SECURITY CLASSIFICATION UNCLASSIFIED		
22a. NAME OF RESPONSIBLE INDIVIDUAL Lucyshyn, William			22b. TELEPHONE NUMBER (Include Area Code) (513) 255-5533		22c. OFFICE SYMBOL AFIT/ENA

19. Abstract

This study evaluates the potential of a newly constructed high pressure proportional counter for the detection of radioactive noble gases. The detector was constructed from stainless steel and machinable ceramic, incorporating design recommendations from a previous study. A new gas handling system was designed and constructed, incorporating a convective flow purification tube filled with calcium turnings.

External sources were used to characterize the performance of the detector using pure argon, argon quenched with varying amounts of methane, a binary mixture (80:20) of argon and xenon, and pure xenon as fill gases. Resolutions were measured as a function of anode voltage and then intrinsic efficiencies were calculated at the optimum resolutions.

A radioactive gas sample was not evaluated when it was found that the field tubes, as designed, did not eliminate the end effects in the detector causing the multiplication to vary along the length of the anode. Consequently, the resolution with an internal sample would not be adequate to perform the required analysis. Additionally, the purification process did not reduce the level of impurities in the available grade of xenon (99.9% pure) to produce useable spectra. Installation of new field tubes, prior to further evaluation of this system, is recommended.

**END**

**FILMED**

**6-85**

**DTIC**